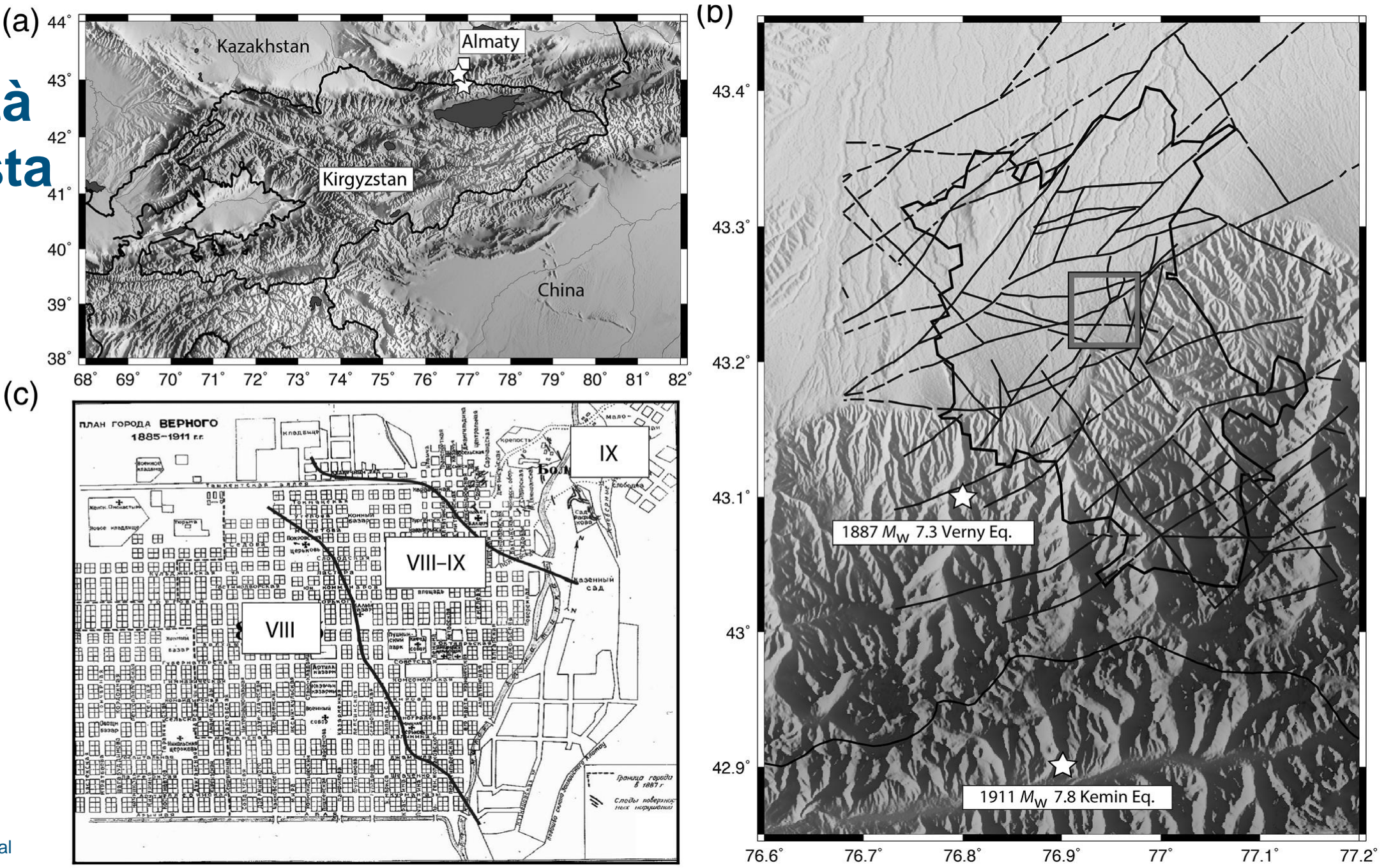


Stagionalità della risposta di sito?



Alshembari et al
(2020)

Stagionalità della risposta di sito?

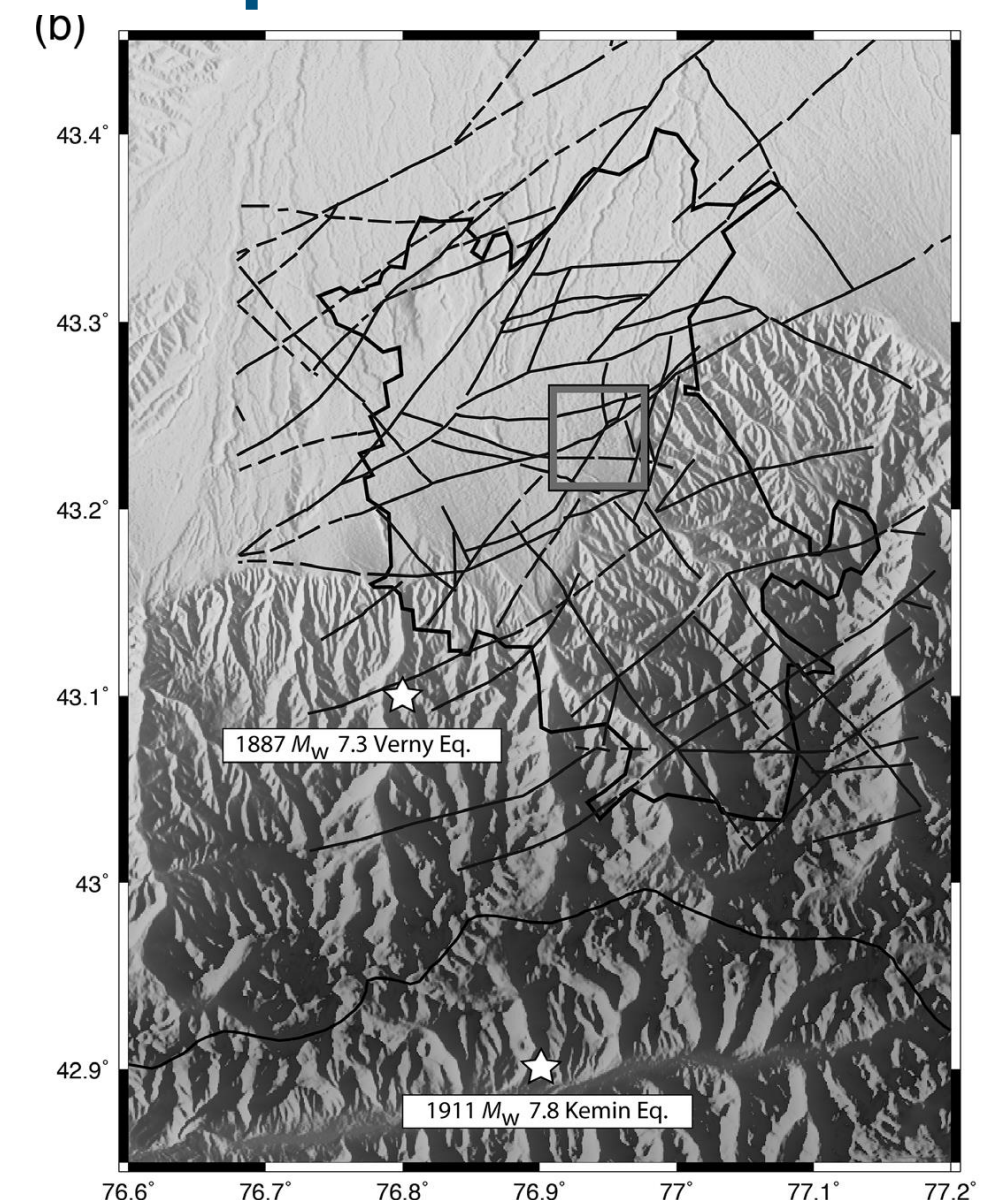
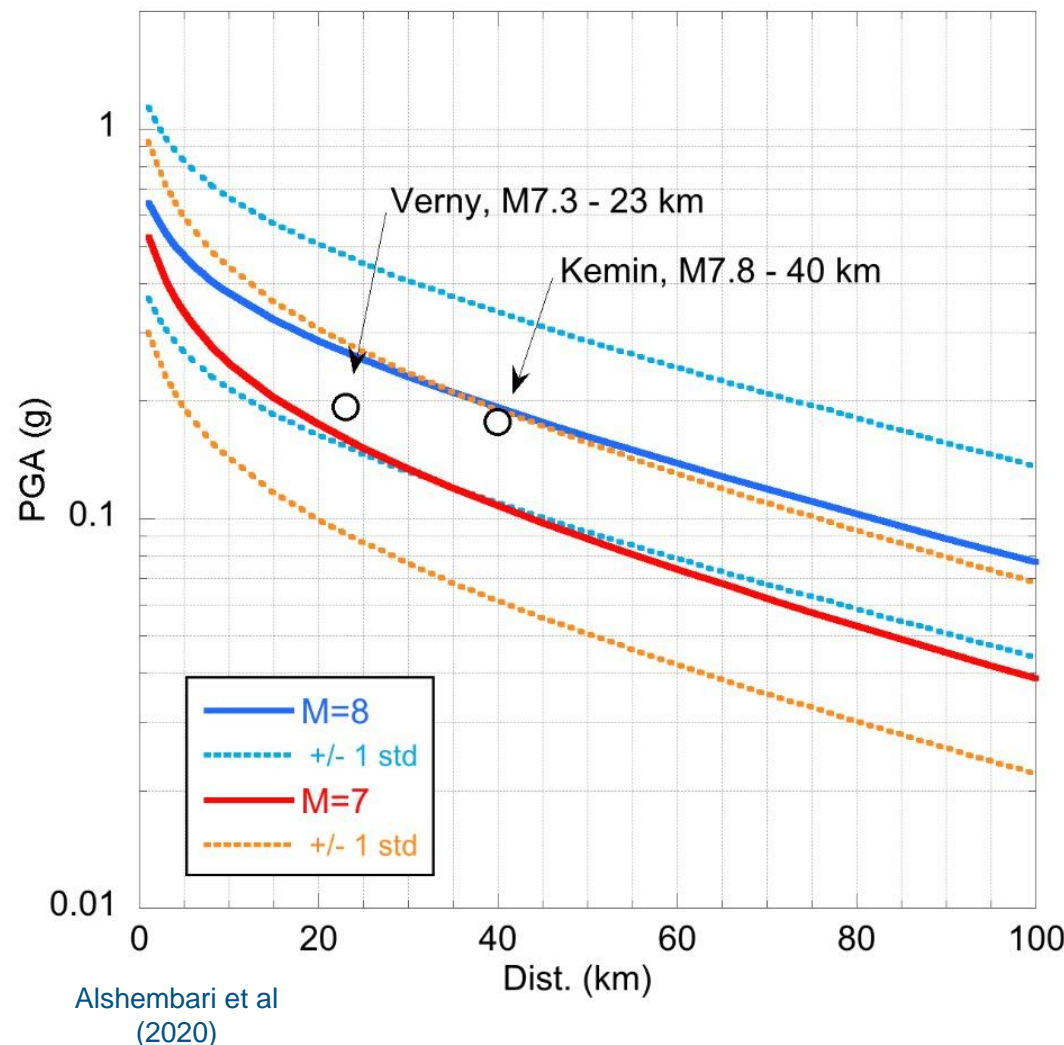
E' possibile che gli effetti superficiali osservati dopo il terremoto del Kemin del 1911 siano stati determinati dalla presenza di uno strato di terreno superficiale ghiacciato, che avrebbe impedito la dissipazione dell'eccesso di pressione di poro verso la superficie e quindi indotto liquefazione?



▲ Figure 2. Ground failure effects documented after the 3 January 1911 Kemin earthquake (modified from [Nurmagambetov et al., 1999](#)).

Stima di possibili effetti di liquefazione

Simili livelli di scuotimento (pga) (Boore and Atkinson, 2008)



Stima di possibili effetti di liquefazione

Ricerca dati sulle caratteristiche del suolo

Ricerca dati di temperatura (da report storici -10°)

Simulazioni fatte con DEEPSOIL per diverse combinazioni dei parametri per tenere conto delle incertezze

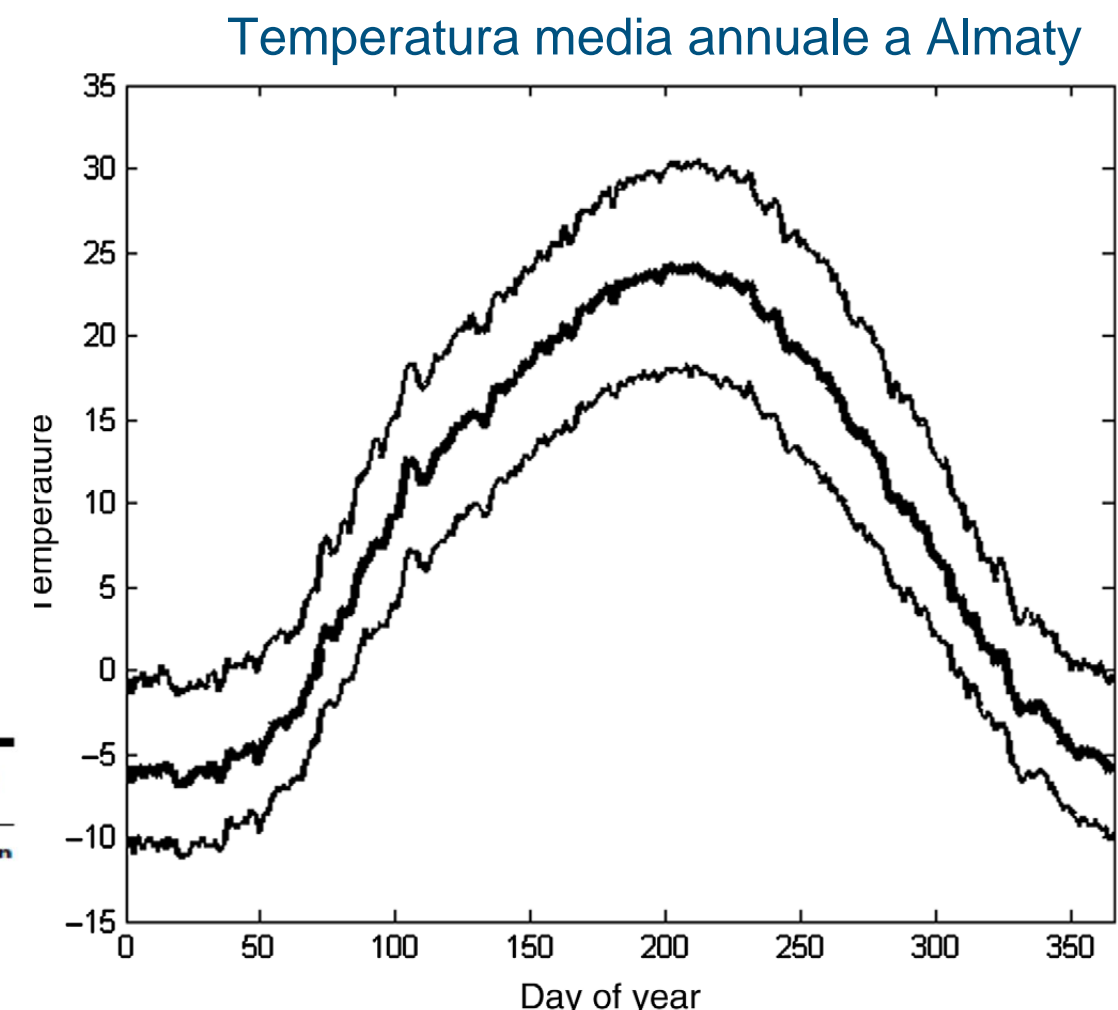
Selezione e scalatura di input sismico per eventi con simile meccanismo, distanza e azimuth rispetto al target

TABLE 1
Typical Values of Vertical Permeability and the Consolidation Coefficient (Pestana et al., 1997; Carlton, 2014) Considered in This Study

Soil Typical Names	Fine Content Percent (%)	Vertical Permeability (m/s)	Consolidation Coefficient
Clayey sands, sand-silt mixtures or silty sands, sands silt mixtures	12 < FC < 50	3×10^{-5}	0.0612
Poorly graded sand with clay	5 < FC < 12	8×10^{-5}	0.1632
Poorly graded sands or well-graded sand	FC < 5	5×10^{-4}	1.02
Gravels	FC = 0	5×10^{-2}	10.2

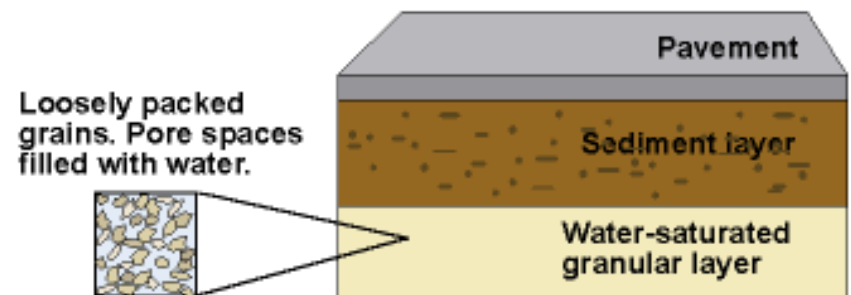
FC, percentage of fine content.

Alshembari et al
(2020)

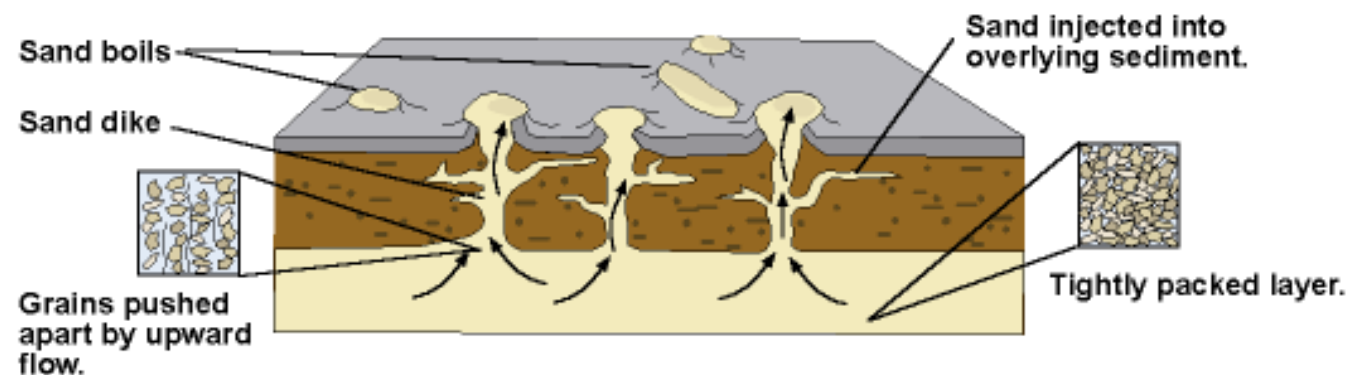


Liquefazione

Before the earthquake



During the earthquake



EARTHQUAKE-INDUCED LIQUEFACTION



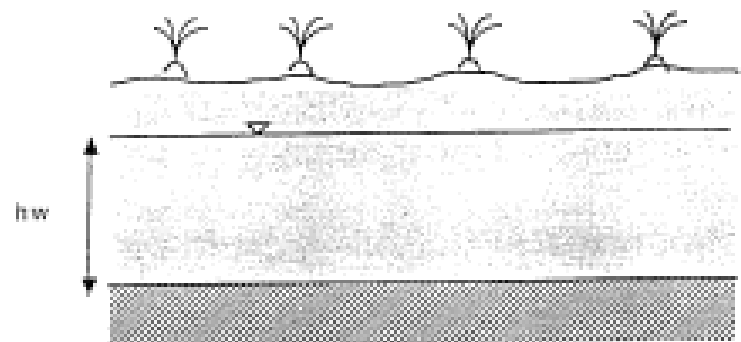
(Image from <http://hirutkonkong1982.spaces.live.com/>)

Liquefaction is characterized by a complete loss of shear resistance

http://www.marum.de/Benjamin_Schlue.html

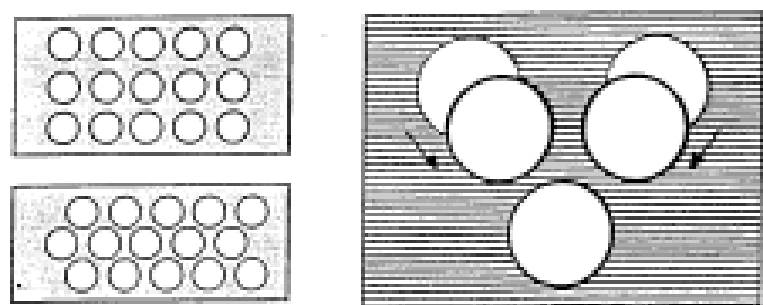
Liquefazione

LIQUEFACTION



cyclical shear

- ⇒ compaction of grains
- ⇒ pore pressure (u) increases



$$S = C + (\sigma - u) \operatorname{tg} \phi$$

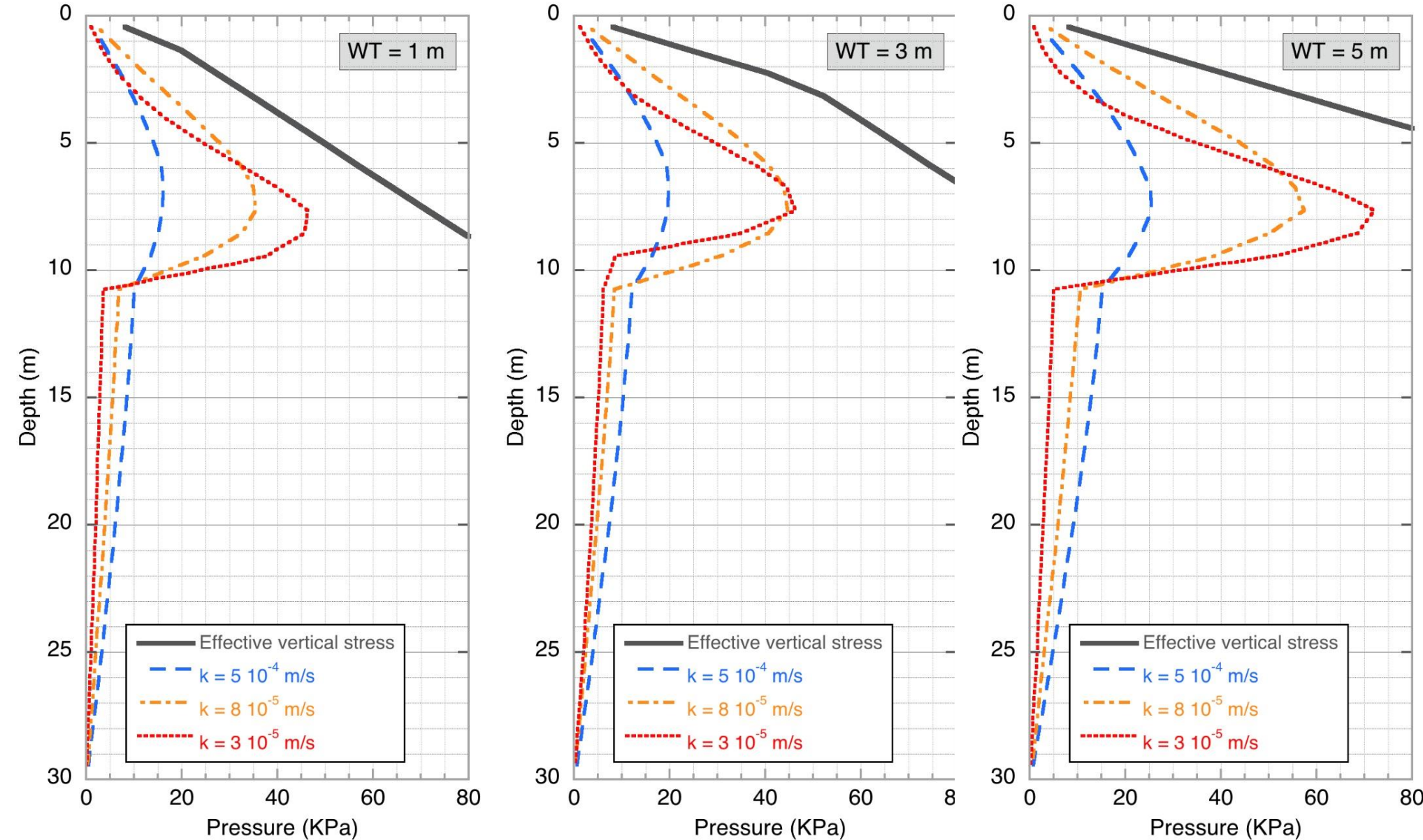
$$\text{si } c = 0 \longrightarrow S = (\sigma - u) \operatorname{tg} \phi$$

$$\text{si } u = \sigma \longrightarrow S = 0$$

- ⇒ effective stress decay
- ⇒ shear strength decay
($\tau_{\max} = \sigma' \cdot \operatorname{tg} \phi'$)

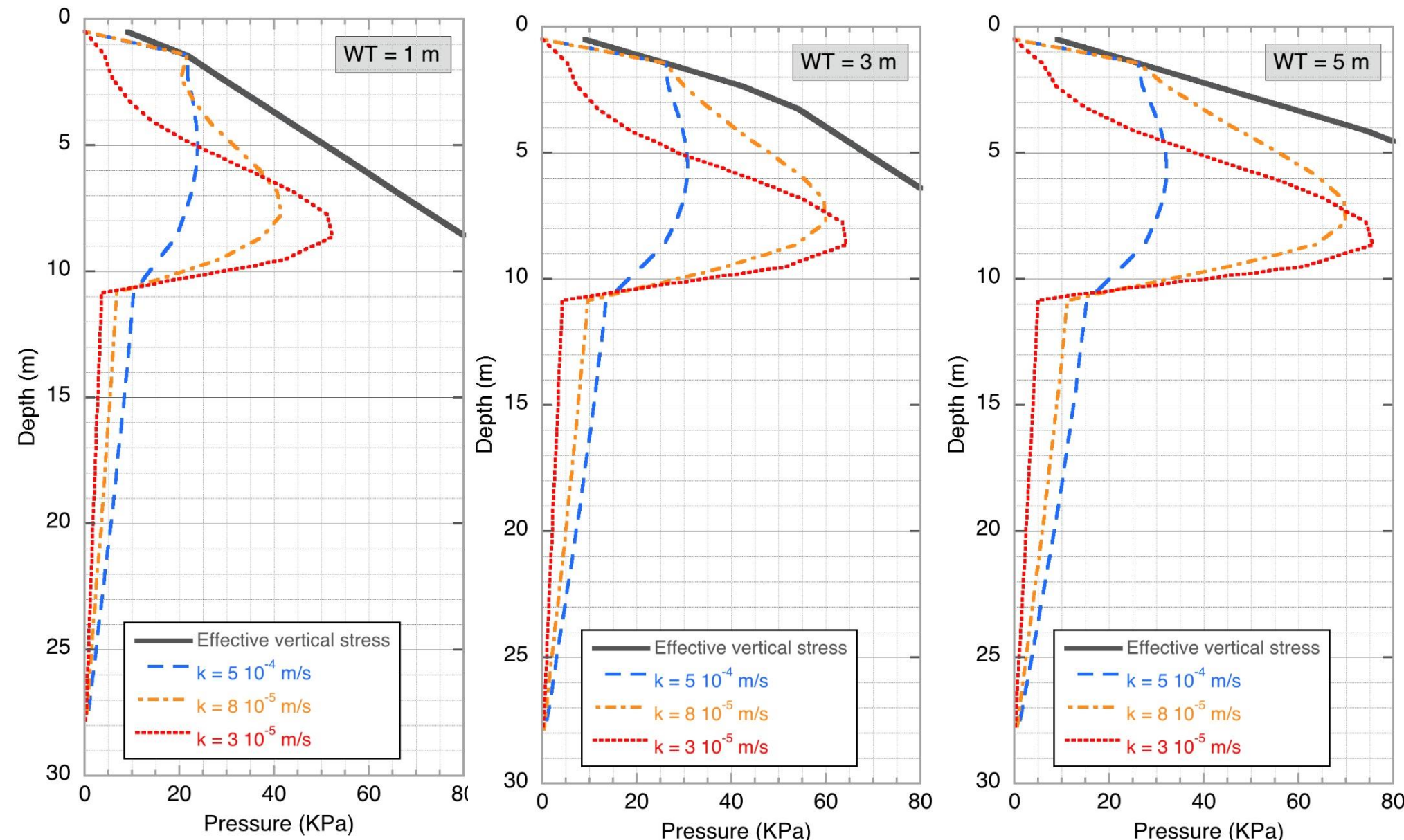
u is the pore pressure
 S the shear resistance
 σ' is the effective stress

Massima Pressione di Poro vs Profondità: profilo di VS “estivo”



Alshembari et al
(2020)

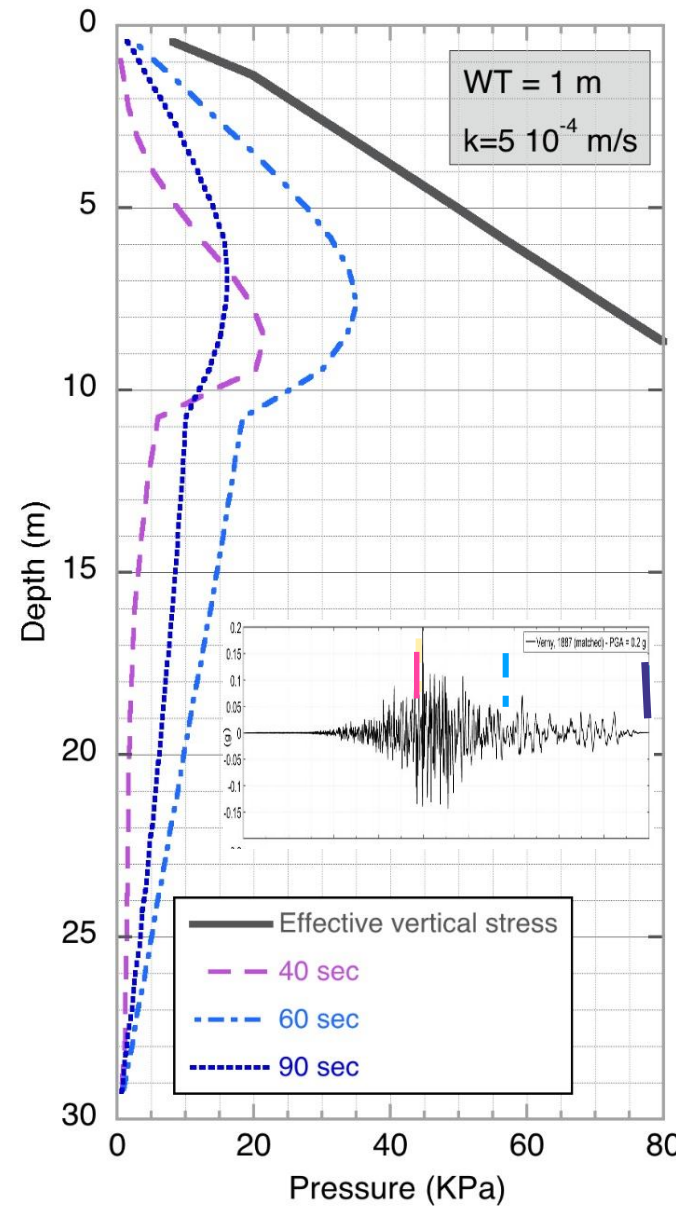
Massima Pressione di Poro vs Profondità: profile di VS “invernale”



Alshembari et al
(2020)

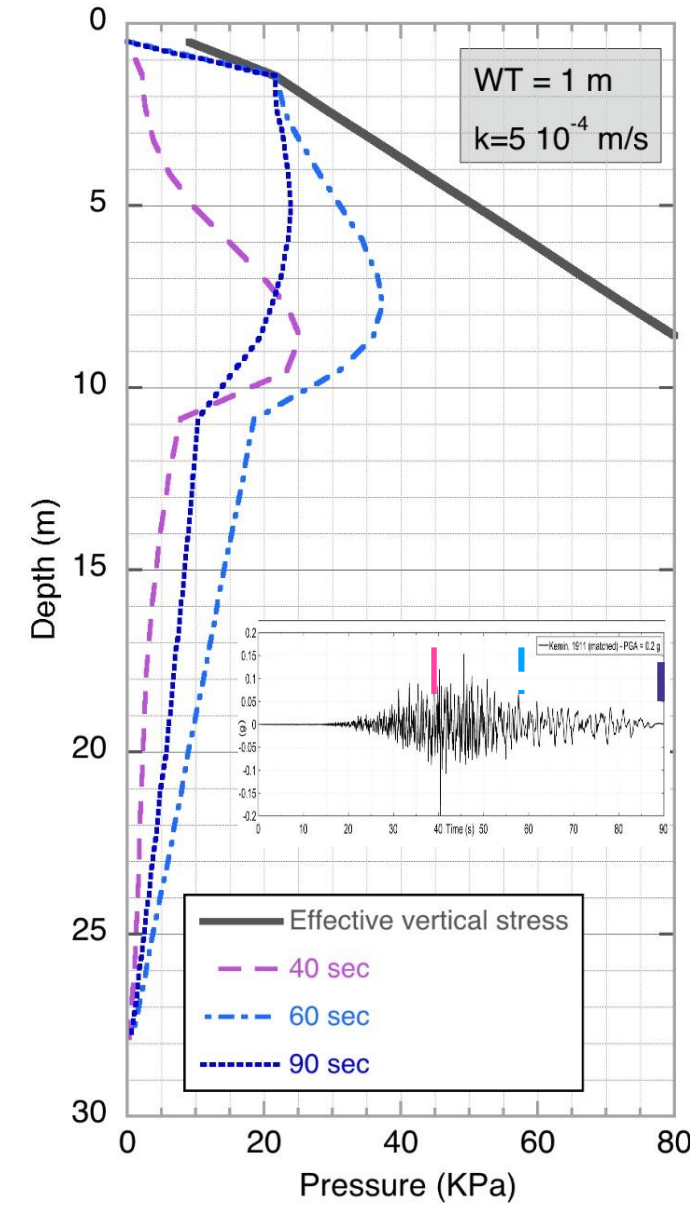
Incremento della pressione di poro a diverse profondità

Verny e profilo estivo



Alshembari et al
(2020)

Kemin e profilo invernale

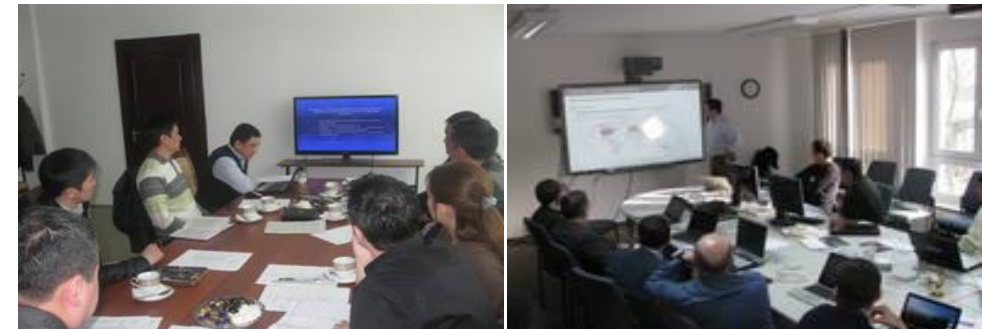


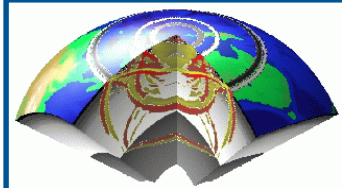
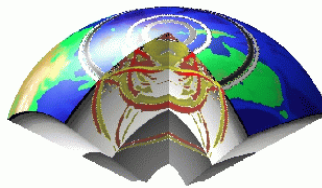
Cooperazione e trasferimento della conoscenza

Stretta cooperazione con gli utilizzatori finali



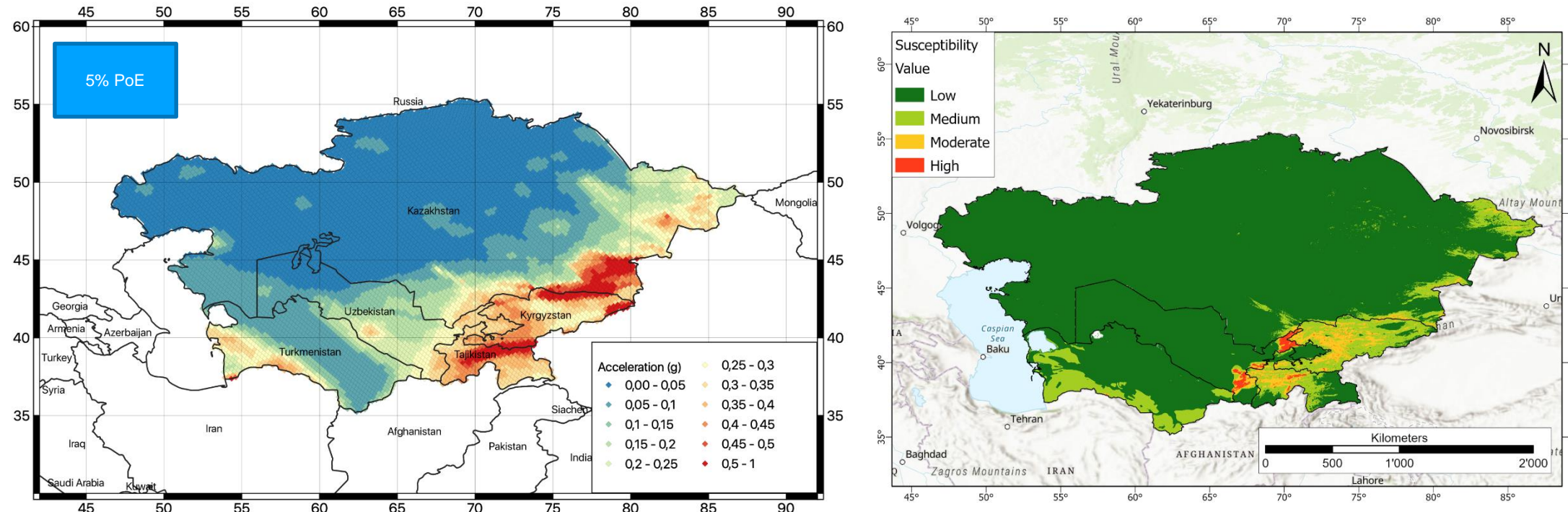
Trasferimento della conoscenza, corsi, esercitazioni





Project “Regionally consistent risk assessment for earthquakes and floods and selective landslide scenario analysis for strengthening financial resilience and accelerating risk reduction in Central Asia”

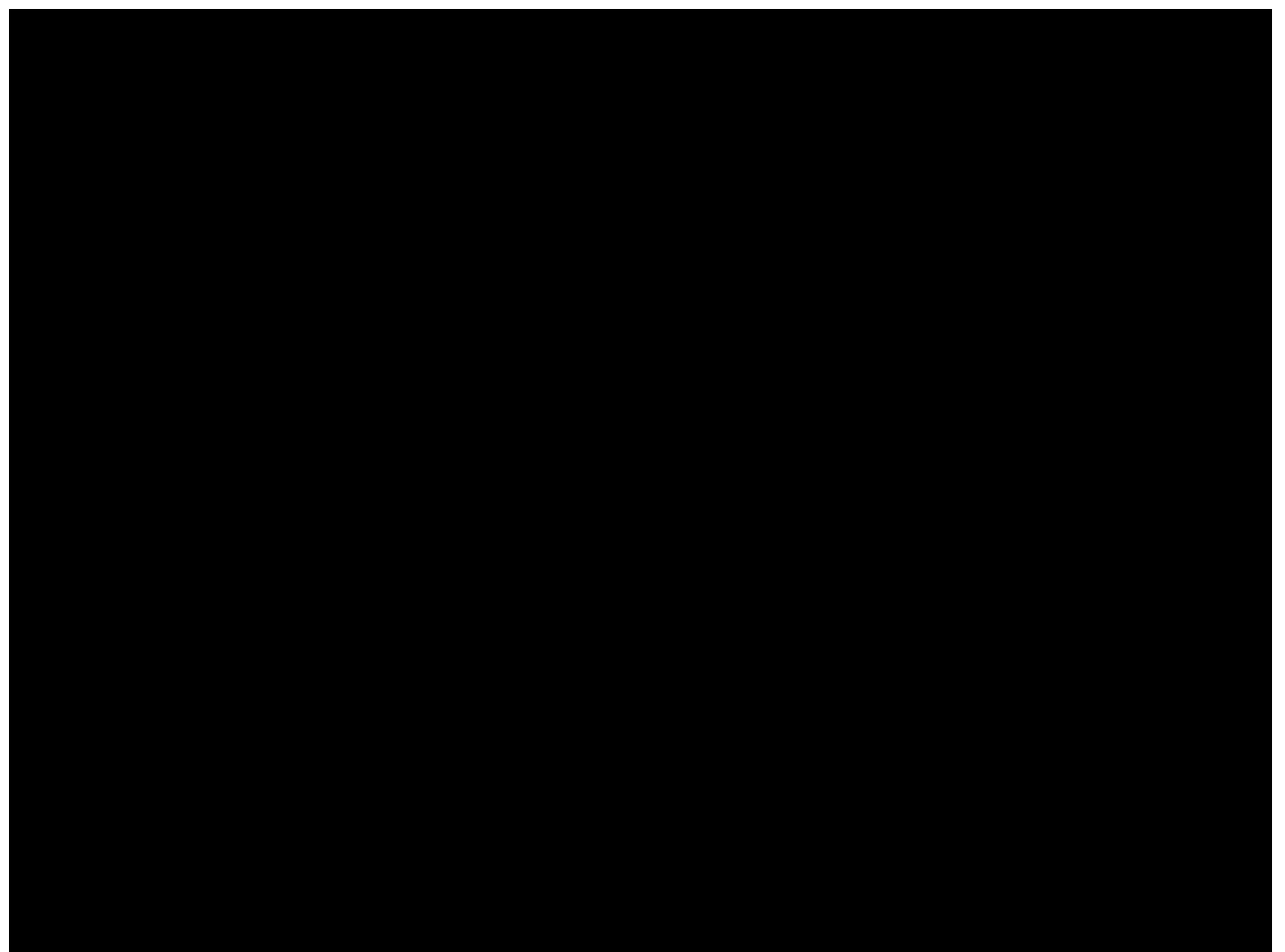
EU-funded Program “Strengthening Financial Resilience and Accelerating Risk Reduction in Central Asia” (SFRARR).



Interventi per prevenzione, preparazione e capacity building



Interventi per prevenzione, preparazione e capacity building



Interventi per prevenzione, preparazione e capacity building



SIBYL

(**S**eismic monitoring and vulnera**B**ilit**Y** framework for civi**L** protection)

Agreement number: ECHO/SUB/2014/695550

<https://www.sibyl-project.eu/welcome-and-project-aims/>

Interventi per prevenzione, preparazione e capacity building



SIBYL

(Seismic monitoring and vulneraBilitY framework for civiL protection)

Agreement number: ECHO/SUB/2014/695550



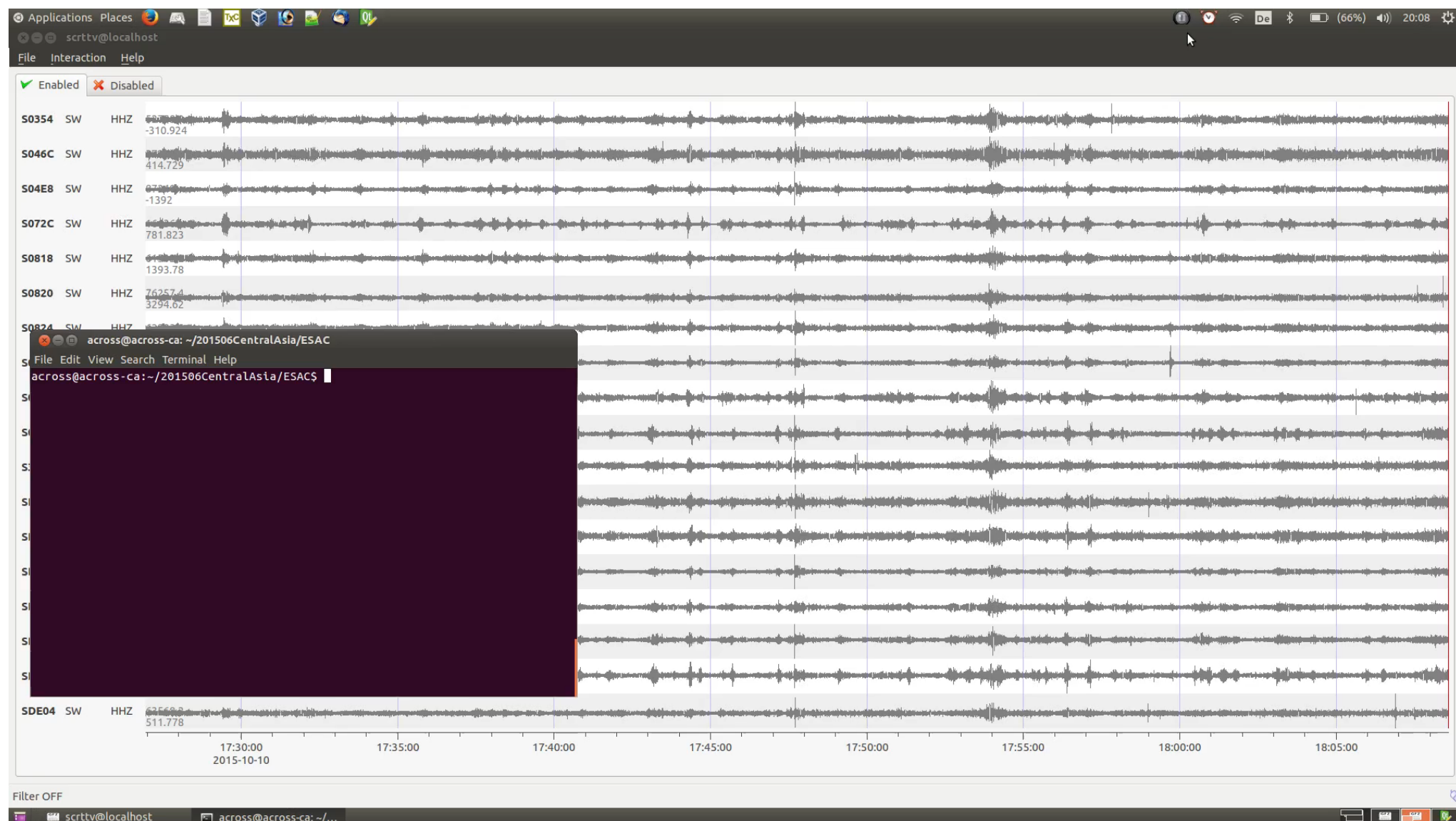
Figure 1: Demonstration of the GFZ-MOMA under development/being expanded upon during the SIBYL project to the attendees of the civil protection workshop.

<https://www.sibyl-project.eu/welcome-and-project-aims/>



Figure 2: Some images of the building surveyed as part of the demonstration of the methods under development within SIBYL.

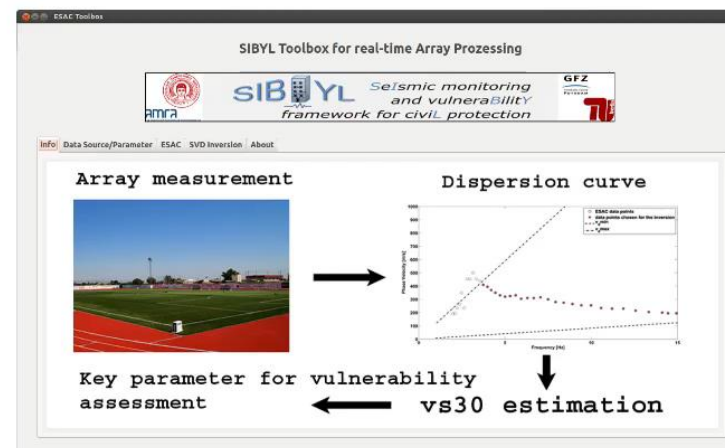
Interventi per prevenzione, preparazione e capacity building



Interventi per prevenzione, preparazione e capacity building



SIBYL Toolbox for real-time Array Processing



amra
■ analysis and monitoring of environmental risk

GFZ
Helmholtz Centre
POTSDAM

TU
berlin

DATA AND EXPERIMENT DESCRIPTIONS

Rapid response seismic networks in Europe: lessons learnt from the L'Aquila earthquake emergency

Lucia Margheriti^{1,*}, Lauro Chiaraluce¹, Christophe Voisin⁴, Giovanna Cultrera², Aladino Govoni^{1,11}, Milena Moretti¹, Paola Bordoni¹, Lucia Luzi³, Riccardo Azzara², Luisa Valoroso¹, Raffaele Di Stefano¹, Armand Mariscal⁴, Luigi Improta², Francesca Pacor³, Giuliano Milana², Marco Mucciarelli⁵, Stefano Parolai⁶, Alessandro Amato¹, Claudio Chiarabba¹, Pasquale De Gori¹, Francesco P. Lucente¹, Massimo Di Bona¹, Maurizio Pignone¹, Gianpaolo Cecere¹, Fabio Criscuoli¹, Alberto Delladio¹, Valentino Lauciani¹, Salvatore Mazza¹, Giuseppe Di Giulio², Fabrizio Cara², Paolo Auglieri³, Marco Massa³, Ezio D'Alema¹, Simone Marzorati¹, Monika Sobiesiak^{6,12}, Angelo Strollo⁶, Anne-Marie Duval⁷, Pascal Dominique⁸, Bertrand Delouis⁹, Anne Paul⁴, Stephan Husen¹⁰, Giulio Selvaggi¹

¹ Istituto Nazionale di Geofisica e Vulcanologia, Centro Nazionale Terremoti, Rome, Italy

² Istituto Nazionale di Geofisica e Vulcanologia, Sezione Roma 1, Rome, Italy

³ Istituto Nazionale di Geofisica e Vulcanologia, Sezione Milano-Pavia, Milan, Italy

⁴ Université de Grenoble, Institut des Sciences de la Terre, Laboratoire de Géophysique Interne et Tectonophysique, Grenoble, France

⁵ Università della Basilicata, Dipartimento di Strutture, Geotecnica, Geologia Applicata all'Ingegneria, Potenza, Italy

⁶ Helmholtz-Zentrum Potsdam - Deutsches GeoForschungsZentrum GFZ, Potsdam, Germany

⁷ CETE Méditerranée (Centre d'Etudes Techniques de l'Equipement), Laboratoire régional des ponts et chaussées, Nice, France

⁸ BRGM (Bureau de Recherche Géologiques et Minières), Service Aménagement et Risques Naturels, Orléans, France

⁹ Université de Nice-Sophia Antipolis, Institut Geosciences AZUR, Valbonne - Sophia Antipolis, France

¹⁰ ETH Zürich (Eidgenössische Technische Hochschule Zürich), Zurich, Switzerland

¹¹ Istituto Nazionale di Oceanografia e Geofisica Sperimentale - OGS, Sgonico (Trieste), Italy

¹² Christian-Albrechts-Universität zu Kiel, Institut für Geowissenschaften, Kiel, Germany

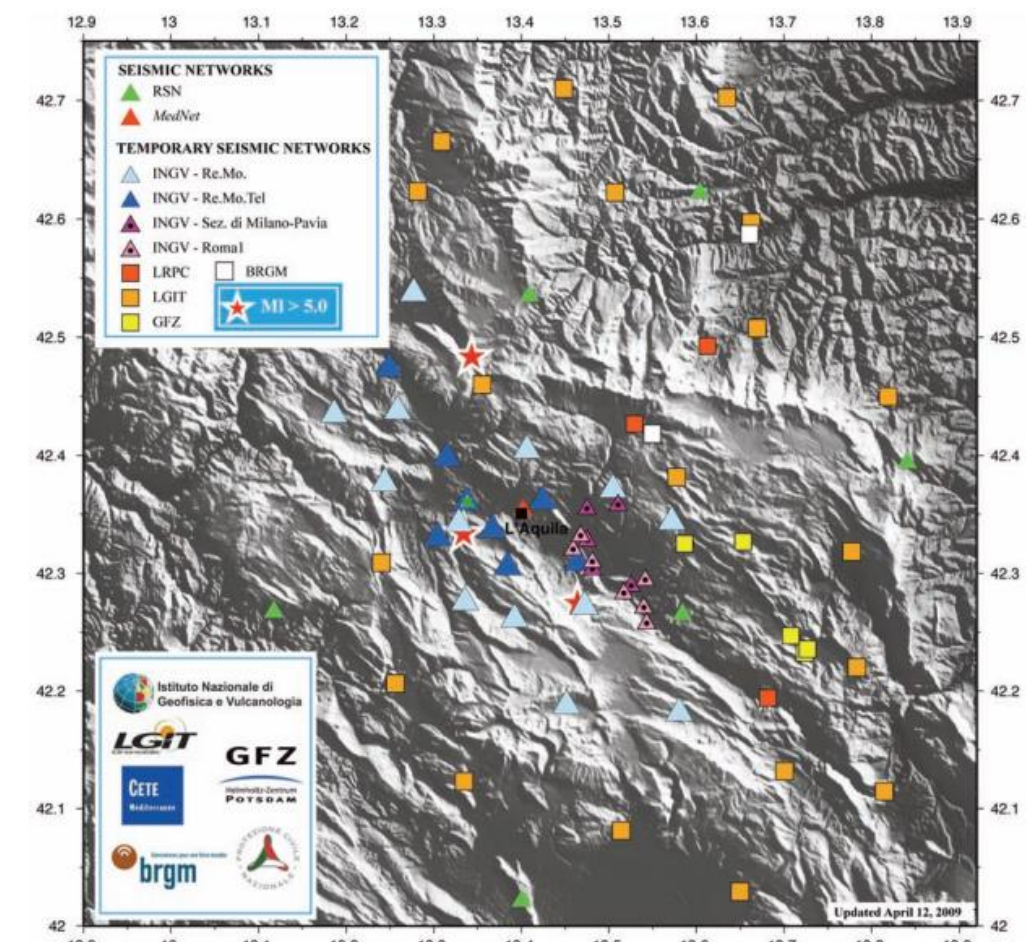


Figure 2. Deployment of the seismic stations during the L'Aquila April 2009 seismic sequence. Several European rapid-response seismic networks took part in the deployment.

Interventi in emergenza

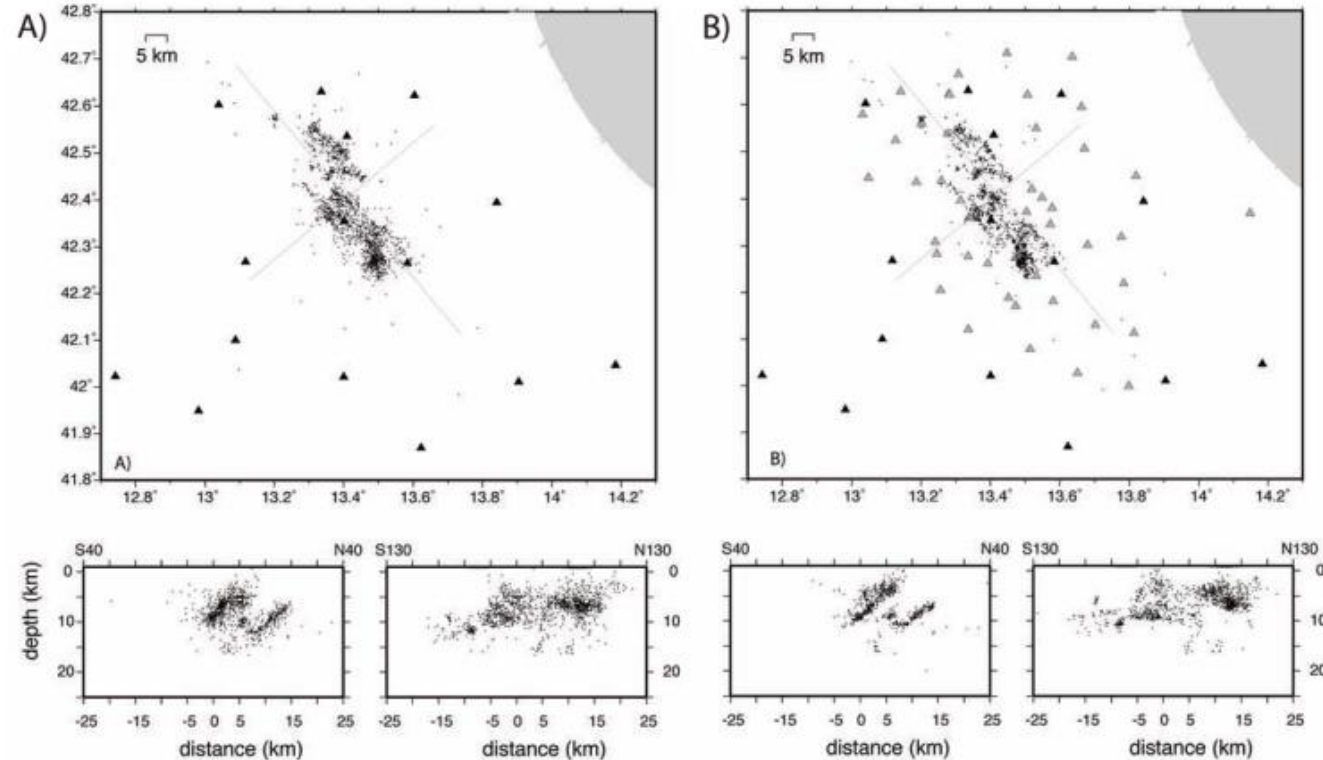


Figure 3. (A) Hypocentral locations using the permanent network (black triangles) for earthquakes with $M > 1.9$ between April and June, 2009. Map above and cross-sections below. The cross sections are reported as two perpendicular grey line in the map. (B) Hypocentral locations using the permanent network (black triangles) and the emergency networks (gray triangles) for earthquakes with $M > 1.9$ between April and June, 2009. Again, map above and cross-sections below. The cross sections are reported as two perpendicular grey line in the map.

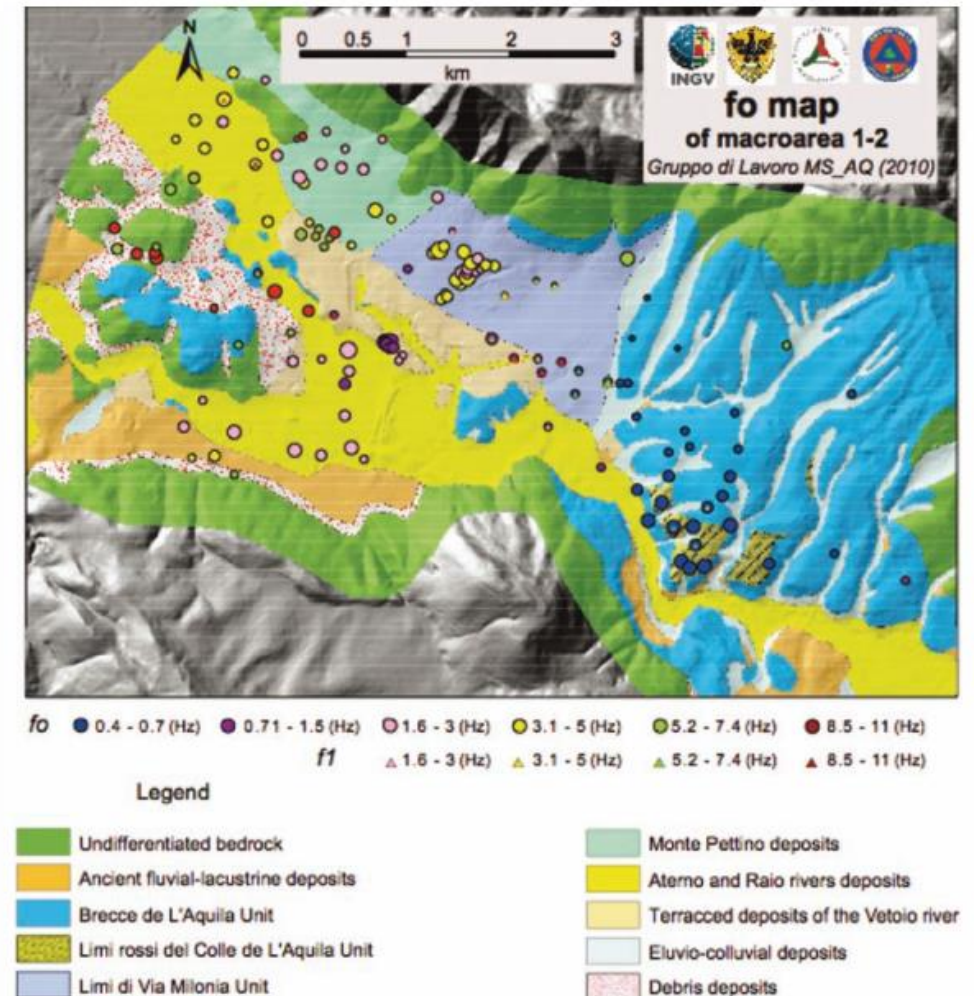


Figure 5. Map showing the fundamental frequencies (f_0) and the second frequency peak (f_1) extracted from the H/V ratios of the seismic noise. The values of f_0 and f_1 are classified into six groups (circles or triangles; different colors; see legend in Figure), with the sizes of the symbols indicative of the amplification amplitude.

Far field damage on RC buildings: the case study of Navelli during the L'Aquila (Italy) seismic sequence, 2009

M. Mucciarelli · M. Bianca · R. D'Amato ·
 M. R. Gallipoli · A. Masi · C. Milkereit · S. Parolai ·
 M. Picozzi · M. Vona

Received: 3 March 2010 / Accepted: 25 July 2010 / Published online: 19 August 2010
 © Springer Science+Business Media B.V. 2010

Abstract After the recent Central Italy Earthquake of the 6th April 2009 ($M_w = 6.3$), the Italian and German engineer and geophysicist Task Force carried out a wide characterization of sites, buildings and damages. In Navelli, a town about 35 km far from epicentre, heavy damage occurred on a reinforced concrete (RC) building that represent an anomalous case of damage, when compared with those occurred in the neighbouring area. In this paper, characterization of the site and damage of the Navelli RC Building is reported and discussed. We performed ambient noise and strong motion measurements, installing one three-directional accelerometer on each floor of the structure and two in free-field, and we have carried out repeated measurements using a couple of three-directional seismometers. In the meantime, a geological survey was carried out and the site response was investigated, with the aid of down-hole measurements. It was thus possible to investigate the structural response and damage taking into account site condition. One of the main results of this work is that repeating analyses using ambient noise measurements show that the main structural frequencies reached after the first damaging shock are constant over time, and then the structural behaviour appears stationary at long term. On the other hand, the strong motion recordings show that the building exhibits a transient non-stationary behaviour as the fundamental frequency changes during each aftershock, then returning to the starting value after each event.

Keywords Earthquake damage · L'Aquila earthquake · Strong motion · Site effects · Building vulnerability · Building monitoring

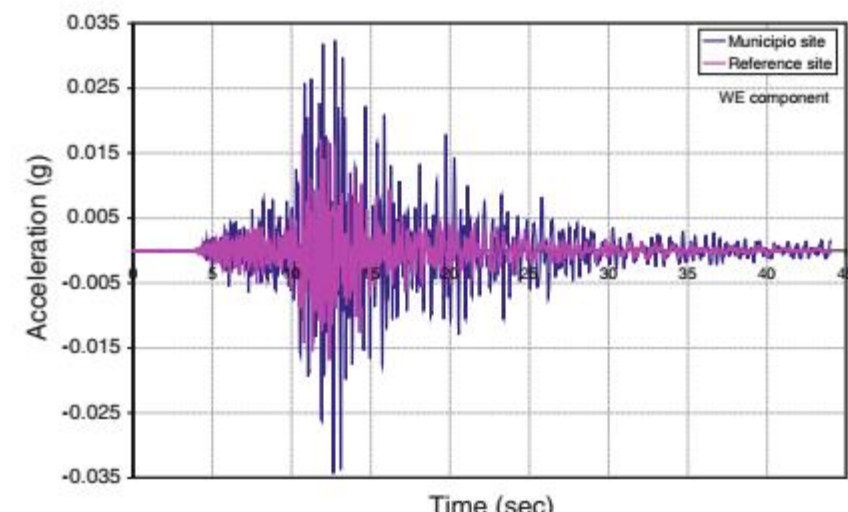
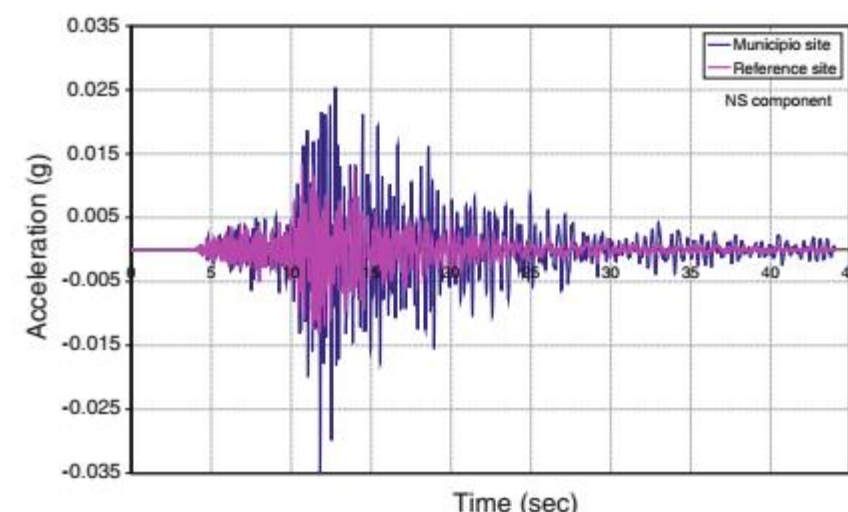
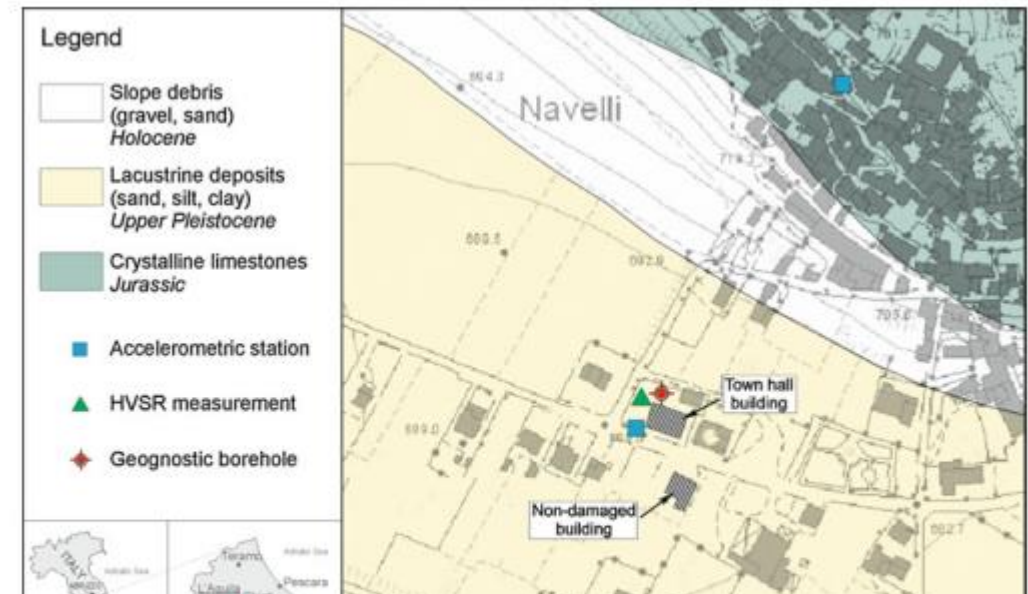


Fig. 3 Comparison between the acceleration recordings of the $M = 5.1$ shock on 9 April at 00.52 a.m. at the town hall (Municipio) and historical centre (Reference site) stations

Article

The Multi-Parameter Wireless Sensing System (MPwise): Its Description and Application to Earthquake Risk Mitigation

Tobias Boxberger ^{1,*}, Kevin Fleming ¹, Massimiliano Pittore ¹, Stefano Parolai ^{1,2}, Marco Pilz ¹ and Stefan Mikulla ¹

¹ Helmholtz Center Potsdam—GFZ German Research Centre for Geosciences, Helmholtzstrasse 7, 14467 Potsdam, Germany; kevin@gfz-potsdam.de (K.F.); pittore@gfz-potsdam.de (M.P.); parolai@gfz-potsdam.de (S.P.); marco.pilz@gfz-potsdam.de (M.P.); stefan.mikulla@gfz-potsdam.de (S.M.)
² Istituto Nazionale di Oceanografia e di Geofisica Sperimentale—OGS, Borgo Grotta Gigante 42/C, 34010 Sgonico (TS), Italy; sparolai@inogs.it
* Correspondence: tobias.boxberger@gfz-potsdam.de; Tel.: +49-331-288-28674

Received: 5 September 2017; Accepted: 18 October 2017; Published: 20 October 2017



Figure 1. A MPwise unit. This version includes a touchscreen embedded in the housing. While this arrangement is not standard, an external touchscreen can be connected to all units. In this image, the touchscreen display shows the operation of the onsite EEW software described in [5–7]. The dimensions of the latest version are: length 20.5 cm, width 16 cm, and height 8 cm.



Figure 4. Example of output from the Seiscomp3 system implemented within the EEW software module of the MPwise, based on the GFZ-Sentry software developed at the GFZ [5–7] for the case of the Kyrgyz Republic. Note that this processing and associated images may be produced by a data center computer connected to the recording network, or on the touchscreen embedded in or connected to one of the units themselves (see Figure 1).

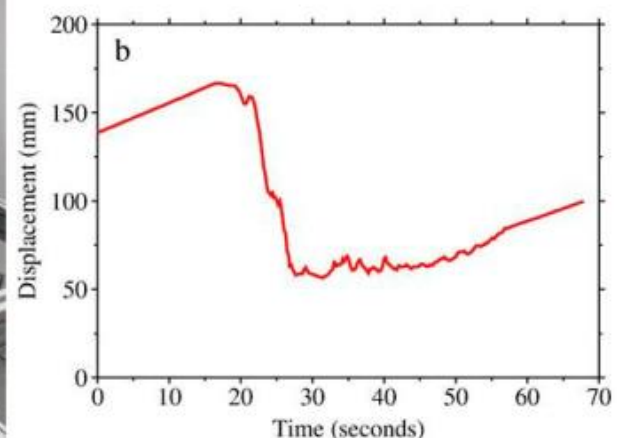
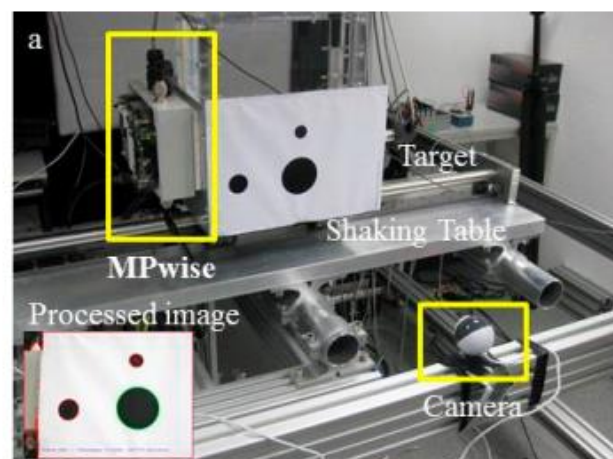


Figure 8. (a) The experimental set-up for the displacement measurements using a camera connected to a MPwise unit; (b) The displacement of the target point (red cross in the processed image in (a)) as determined from the camera images.

Interventi in emergenza

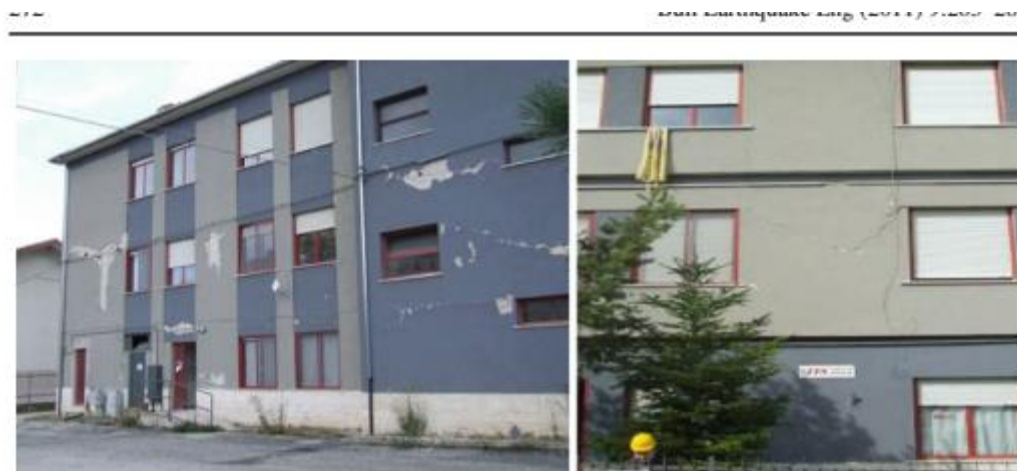


Fig. 9 Damage on infill panels along the X1 and X3 Frames



Fig. 10 Damage on non-structural elements along the X2 frame at the ground and first storeys

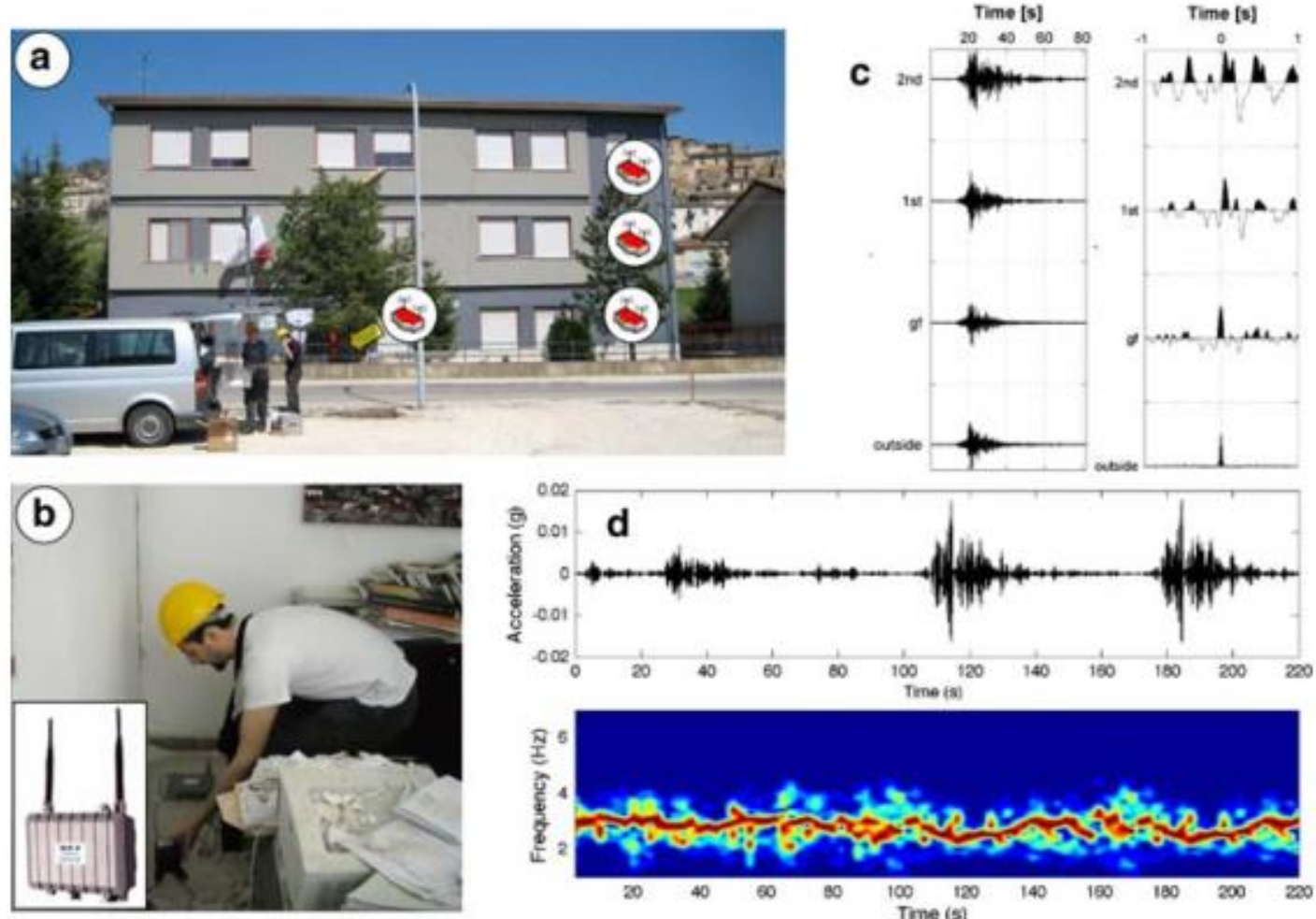
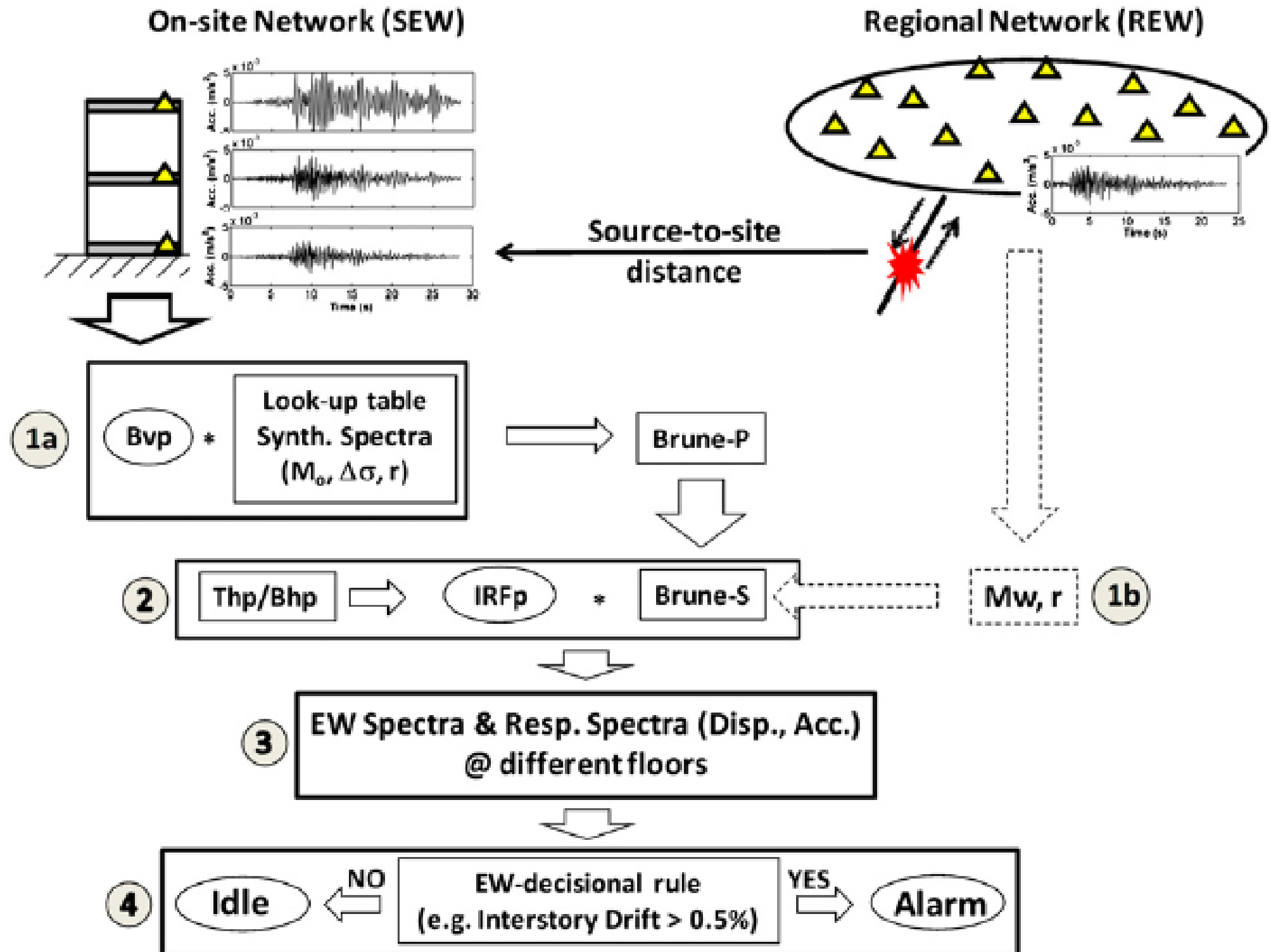


Fig. 1 Real-time monitoring of Navelli's municipality center (L'Aquila, Italy). **a** and **b** Since the 8th April 2009, three wireless accelerometric stations have been installed at the different floors of the Navelli municipality building, with one station deployed outside of it, all recording the sequence of aftershocks following the Mw 6.3 Central Italy Earthquake April 6, 2009. **c** and **d** During the last few weeks, the structure has experienced an increasing amount of damage, with access to within the structure no longer considered possible. Nevertheless, the wireless accelerometers are still operating, hence the earthquake data can still be safely downloaded from outside the building. The deconvolution of accelerometric recordings within the building with a reference one (in this case, the station located outside) allows the monitoring of the transfer function of the structure. The continuous spectral analysis of data (**d**) allows a nearly real-time monitoring of the building's modal property variations and of the level of damage during the occurrence of aftershocks. Note the clear decrease between 100 and 140 s, as well as 170 and 210 s, of the fundamental resonance frequency of the building during the largest amplitude arrivals of the strongest aftershock recordings

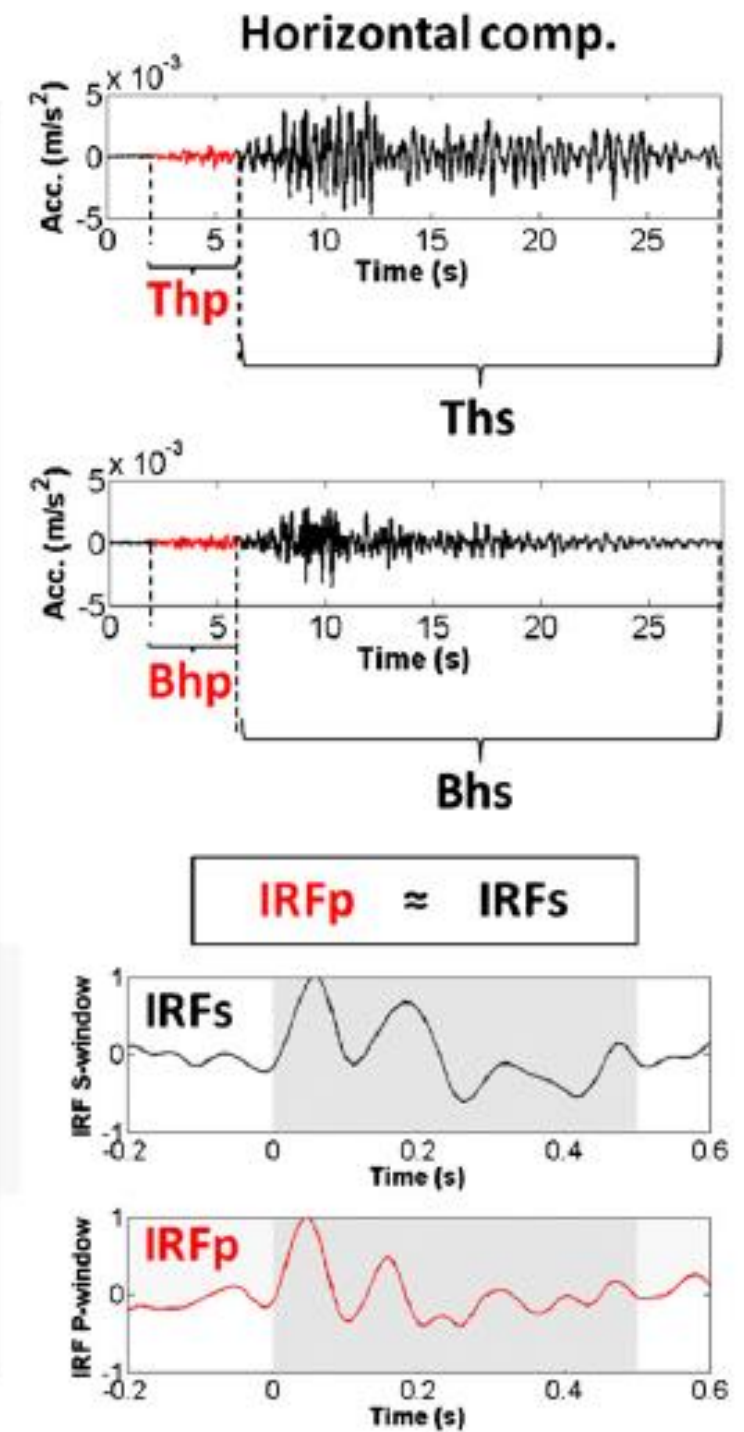
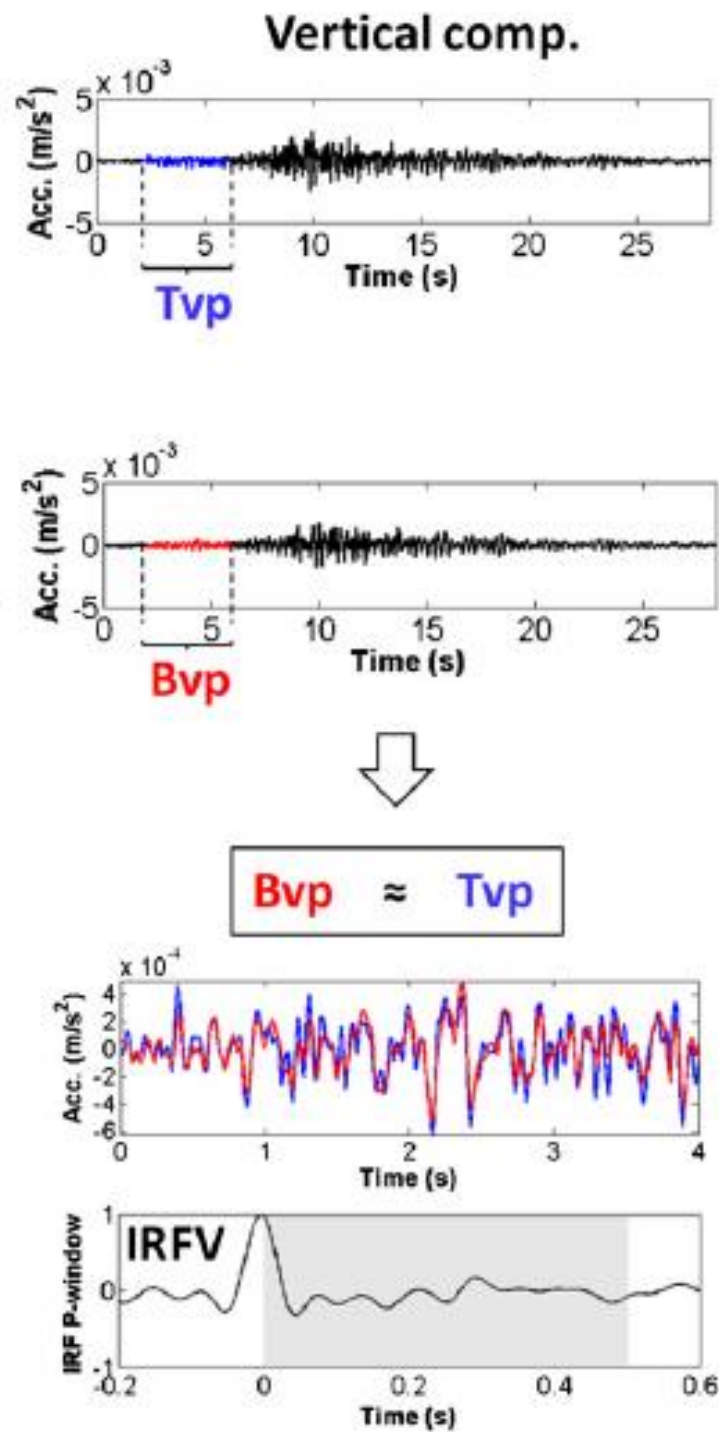
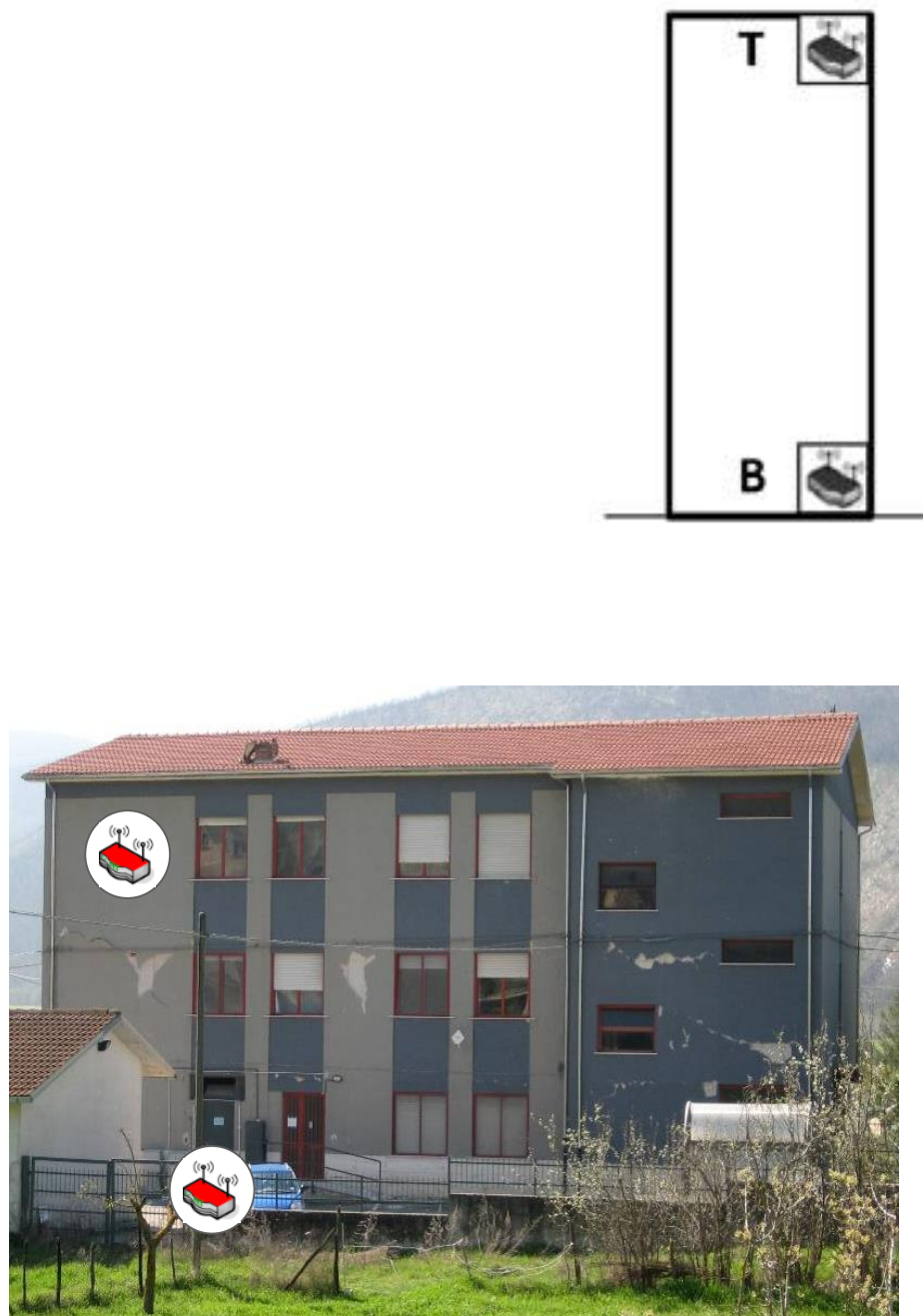
Interventi in emergenza



Picozzi et al., (2011)

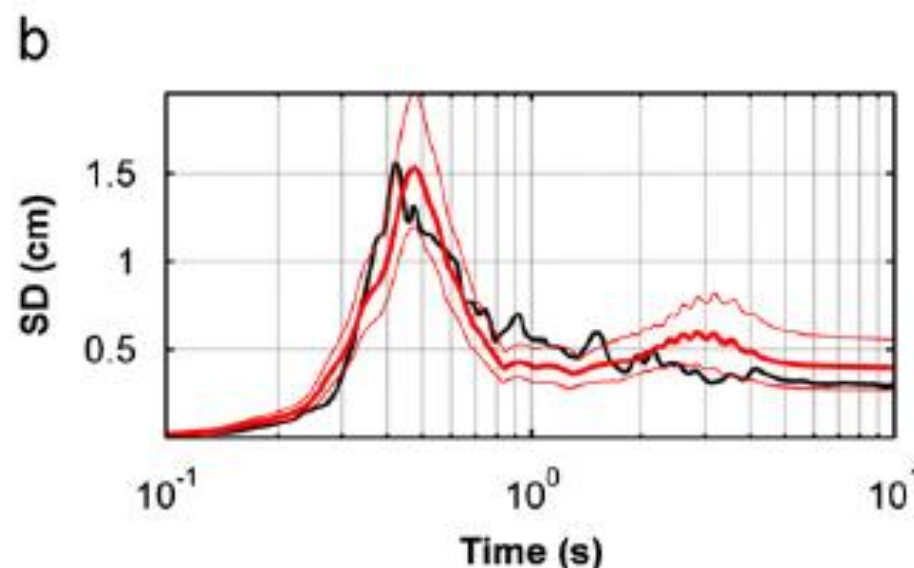
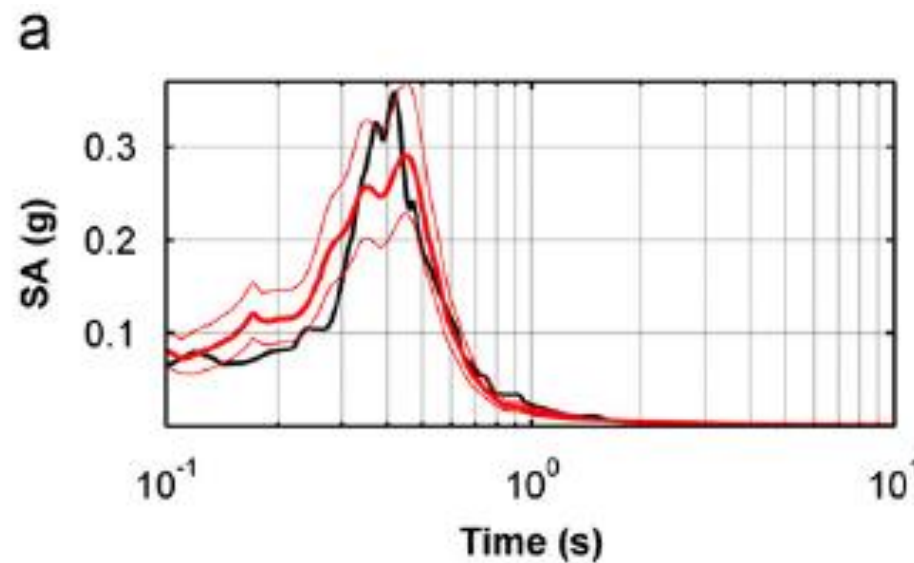
Interventi in emergenza
Early warning and rapid response

Tailor made early warning

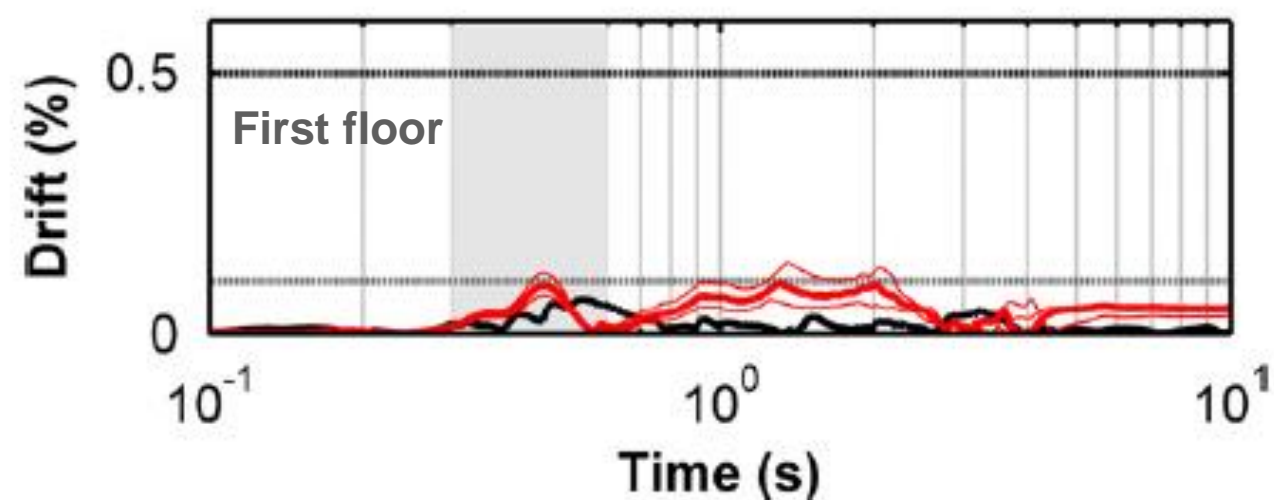
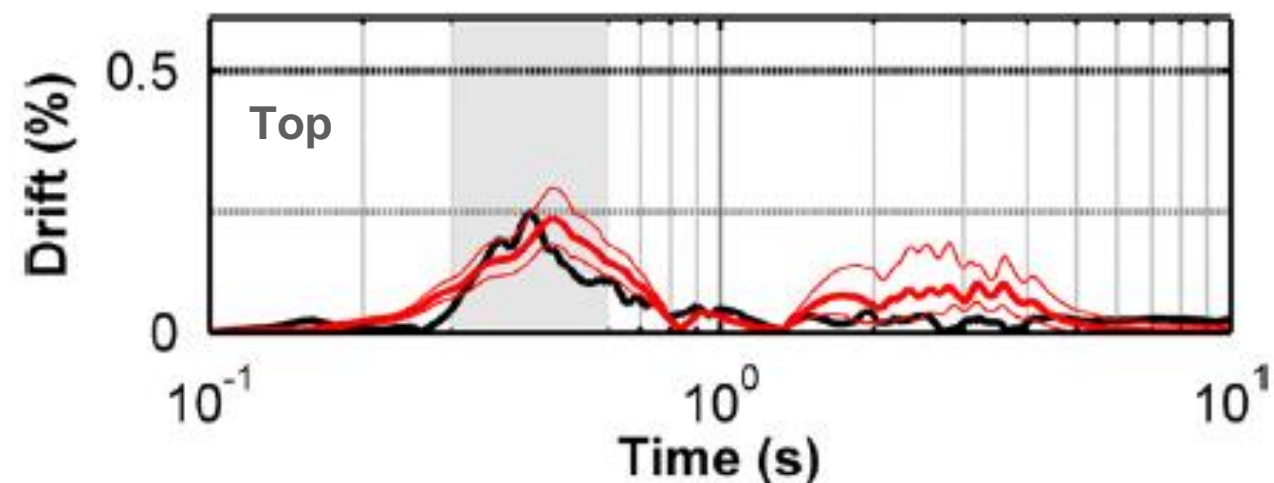


Interventi in emergenza

Estimated (red) and measured (black) response spectra



Estimated (red) and measured (black) inter-storey drift displacement



Interventi in emergenza

Fig. 1 Scheme of the topographic categories and coefficients for the Italian seismic code

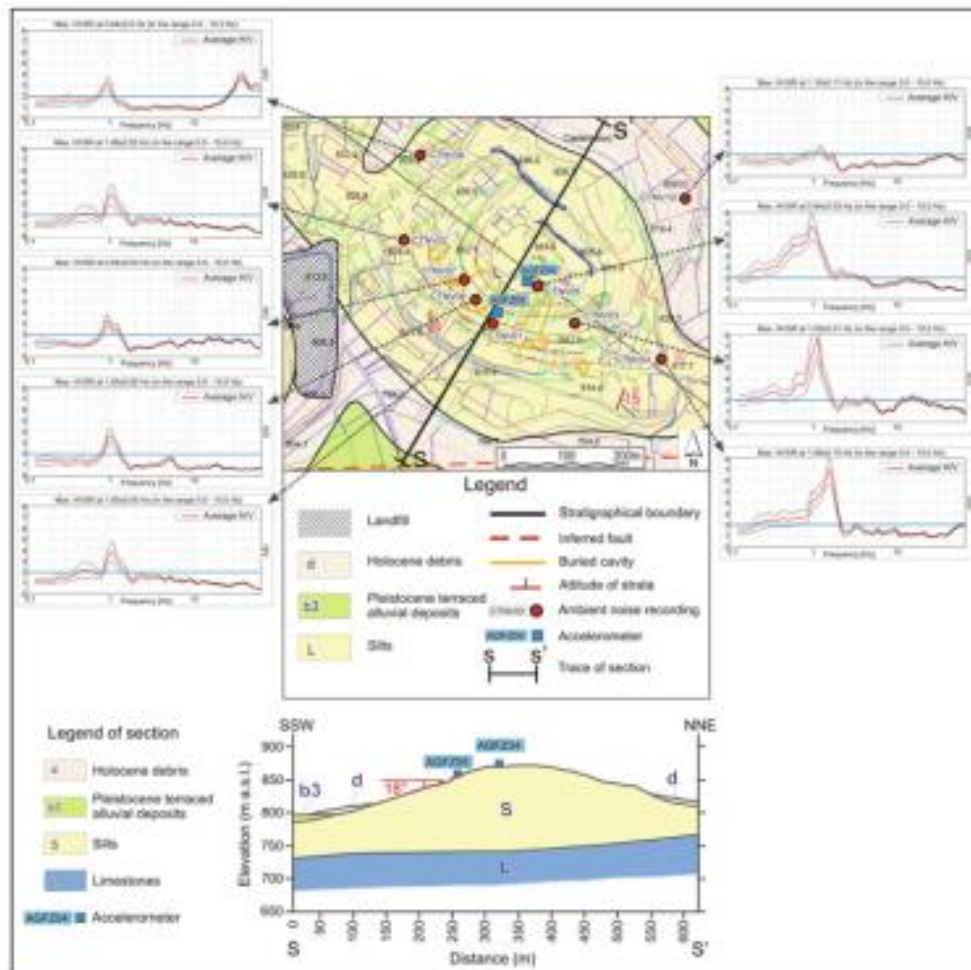


Fig. 2 Geological map and section for Castelnuovo (modified from Gallipoli et al. 2011)

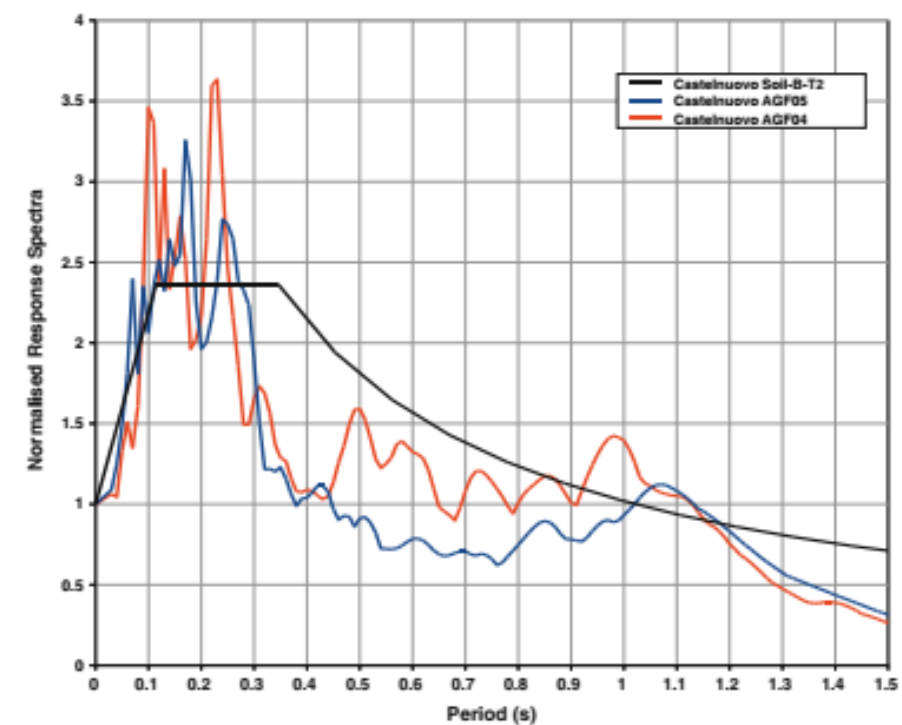
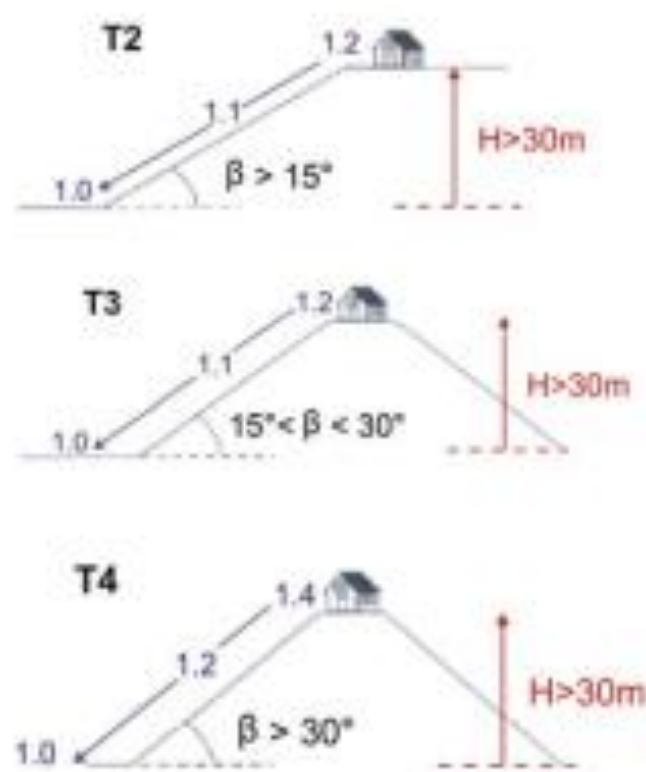


Fig. 5 Normalised Response spectra of the M 5.1 event of April 9, 2009 recorded at two sites in Castelnuovo compared with code provision

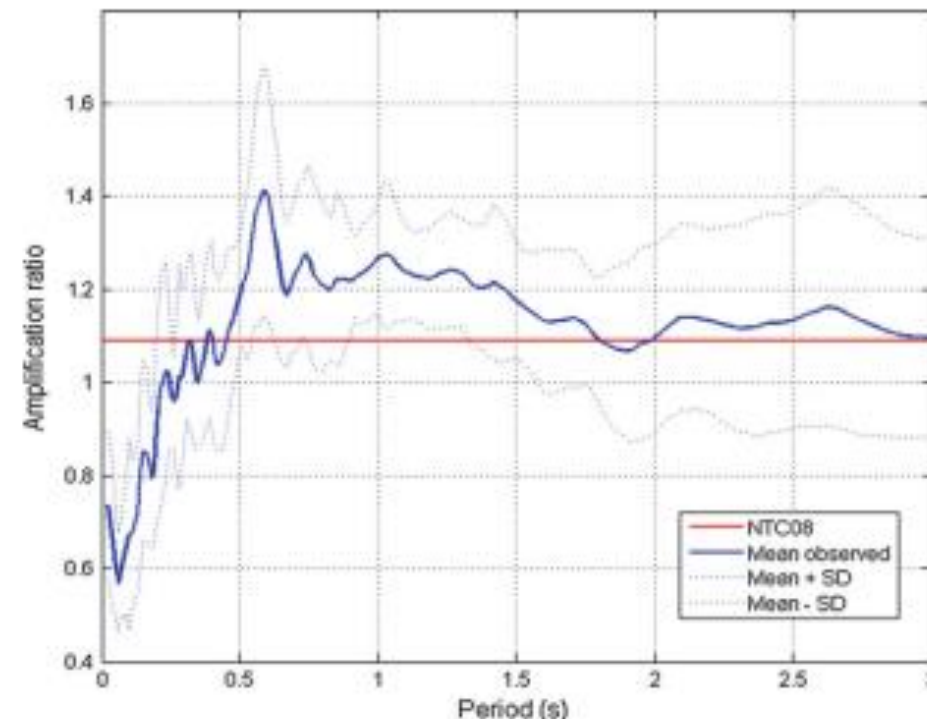


Fig. 6 Comparison between code provisions ratio (red) and observed amplification ratio (blue) in Castelnuovo

Interventi in emergenza

Fig. 1 Scheme of the topographic categories and coefficients for the Italian seismic code

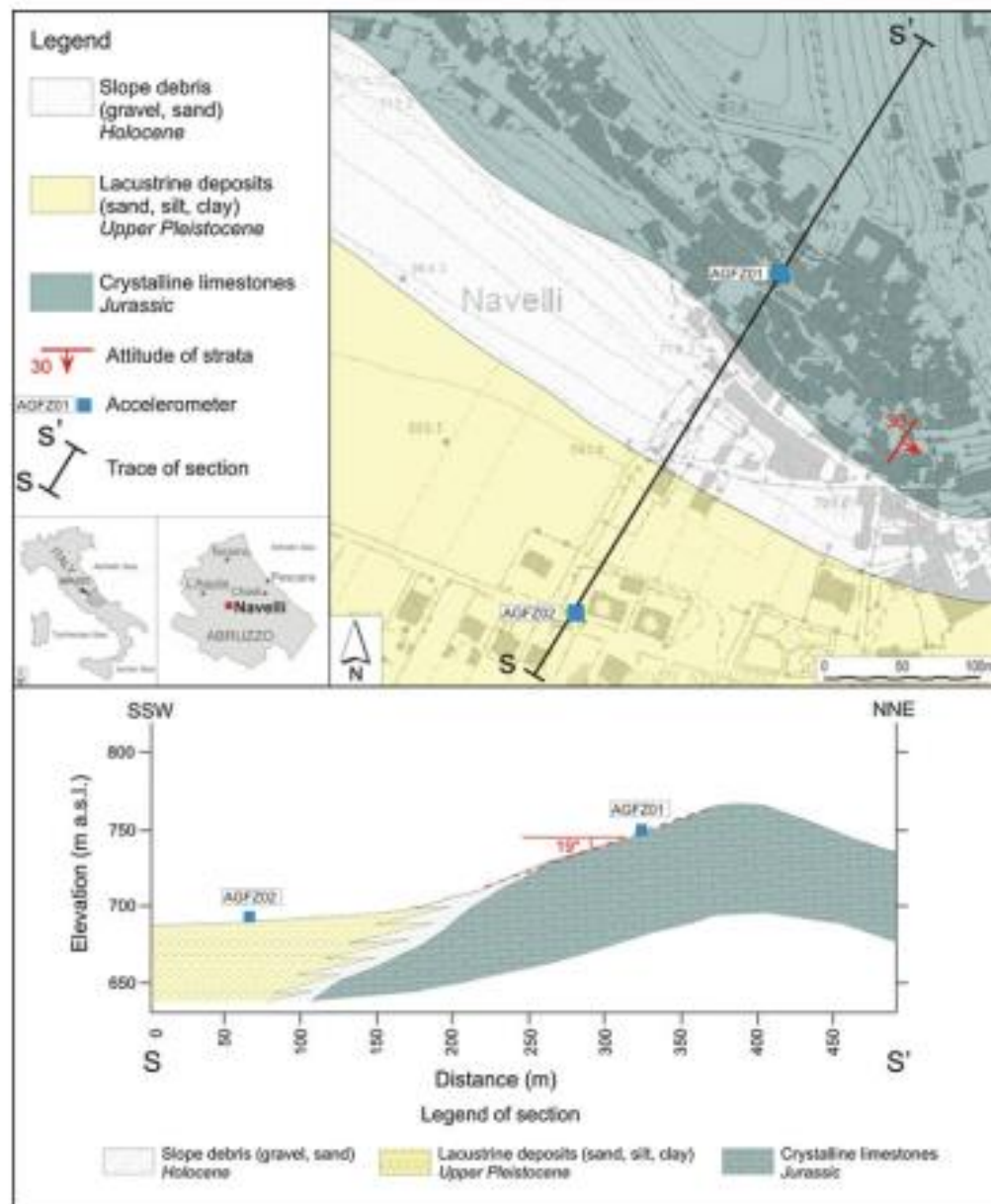


Fig. 7 Geological map and section for Navelli

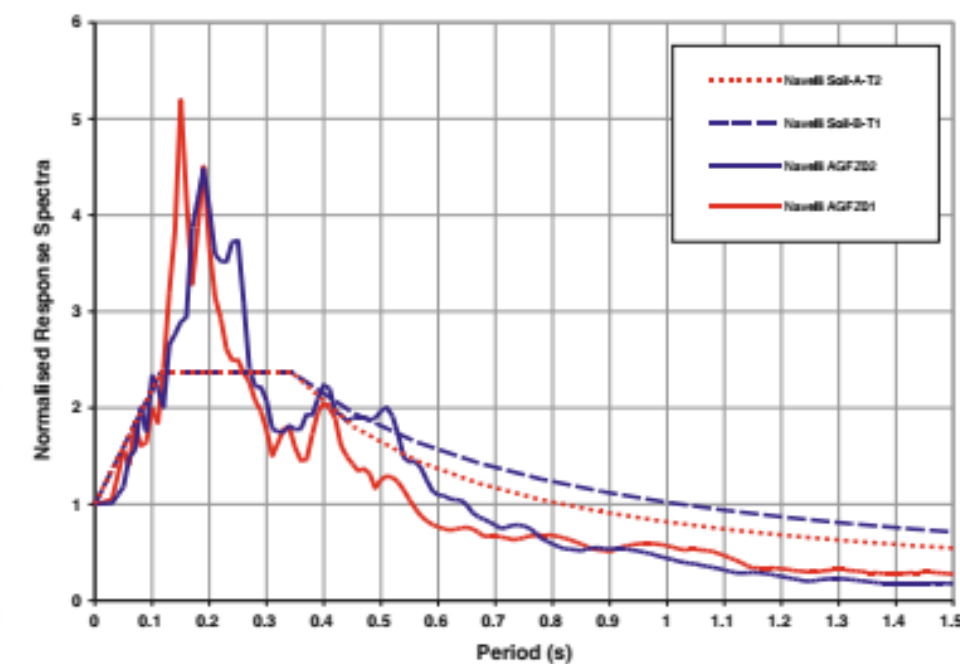
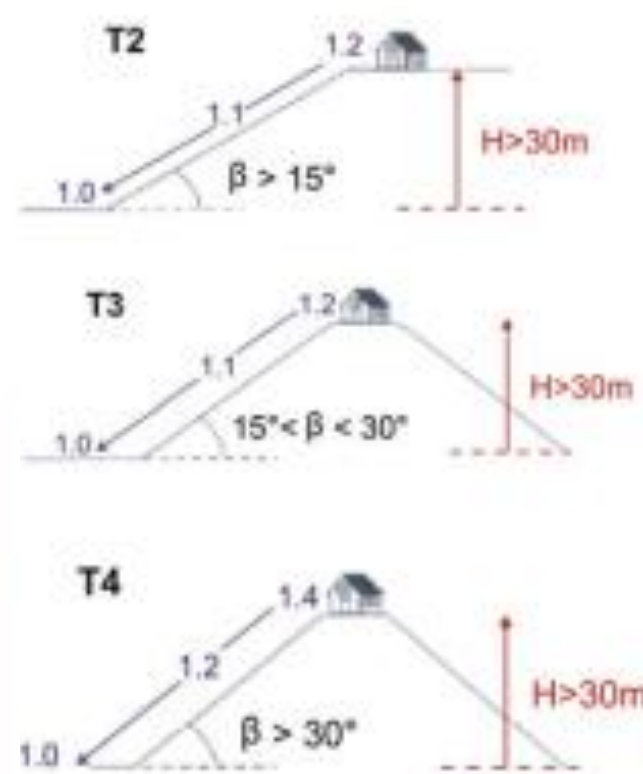


Fig. 10 Normalised Response spectra of the M 5.1 event of April 9, 2009 recorded at two sites in Navelli compared with code provision

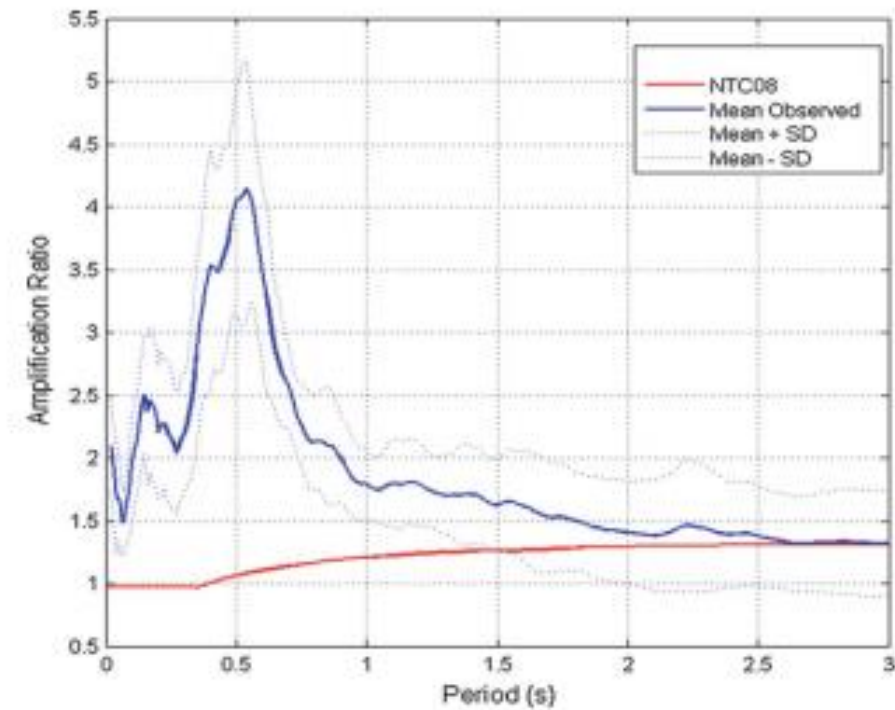


Fig. 11 Comparison between code provisions (red) and observed amplification ratio (blue) in Navelli

Bayesian Estimation of Macroseismic Intensity from Post-Earthquake Rapid Damage Mapping

Massimiliano Pittore,^{a)} Laura Graziani,^{b)} Alessandra Maramai,^{b)}
Michael Haas,^{a)} Stefano Parolai,^{c)} and Andrea Tertulliani^{b)}

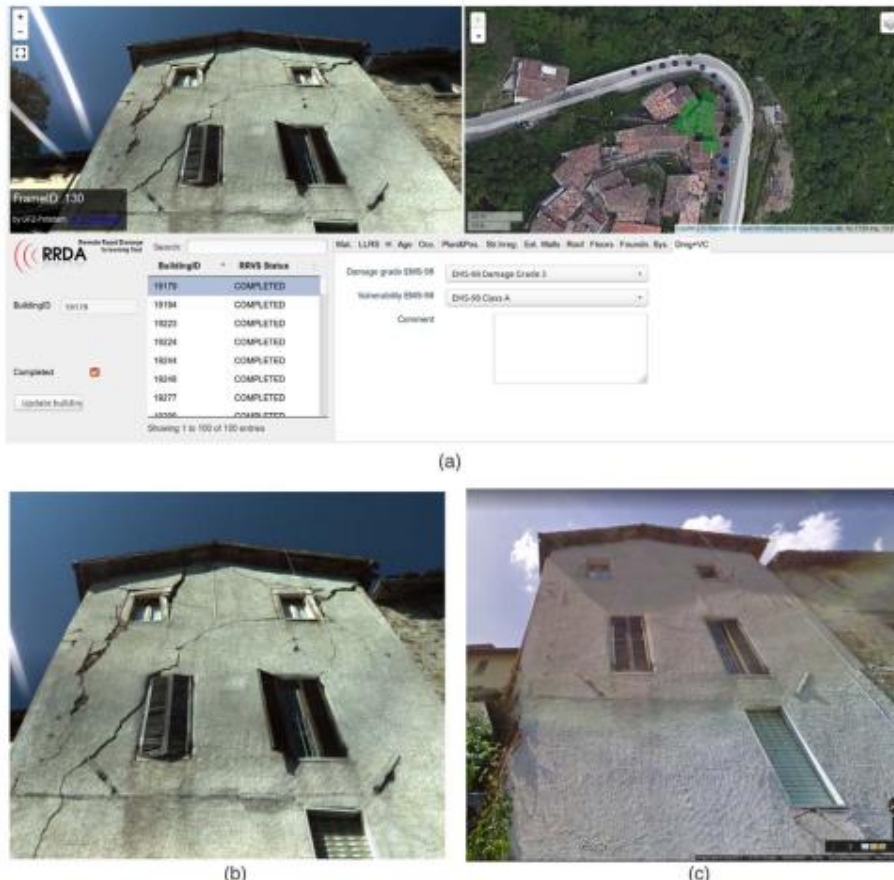


Figure 2. An example of a building selected for inspection and remotely analyzed by surveyors. (a) The RRDA web-based interface showing, on the right side, an aerial map with the selected building (green shading) superimposed and the location of the closest omnidirectional images (blue dots). On the left, the selected omnidirectional image can be zoomed and panned (or visualized full-screen). The lower part of the interface lists the buildings of the task (each building can be selected by clicking on the corresponding item in the list) and the drop-down menus for entering the observed damage and vulnerability class. (b) Omnidirectional image captured by the mobile mapping system. (c) Corresponding pre-event omnidirectional image from the Google StreetView service.

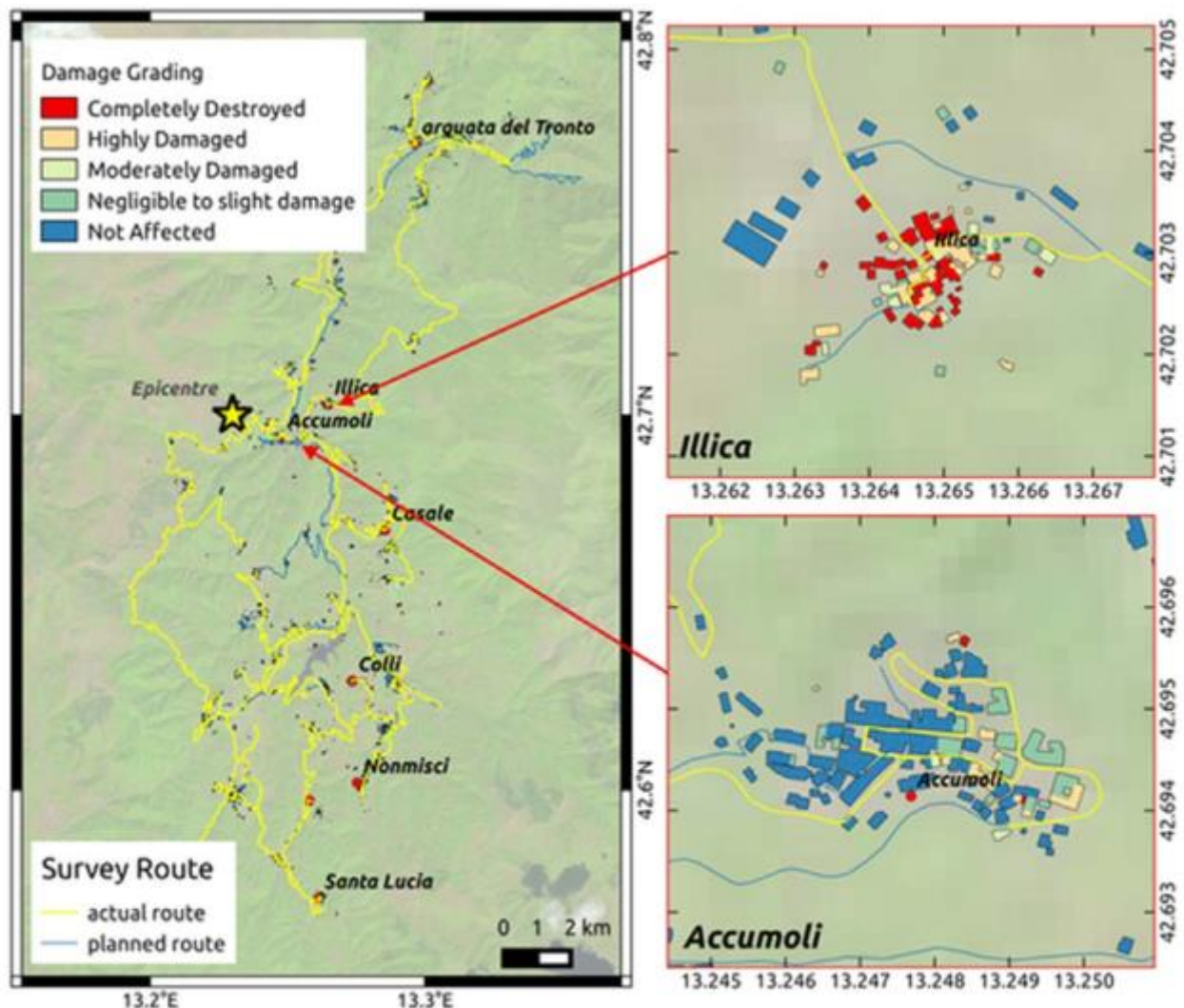


Figure 1. Overview of the study area subjected to grading from the Copernicus Rapid Mapping service. The inset shows a close-up of the building-by-building grading in the towns of Accumoli and Illica (in the Rieti provincial district).

Interventi in emergenza

Progettazione dell'intervento e misure



Interventi in emergenza



Multi hazard



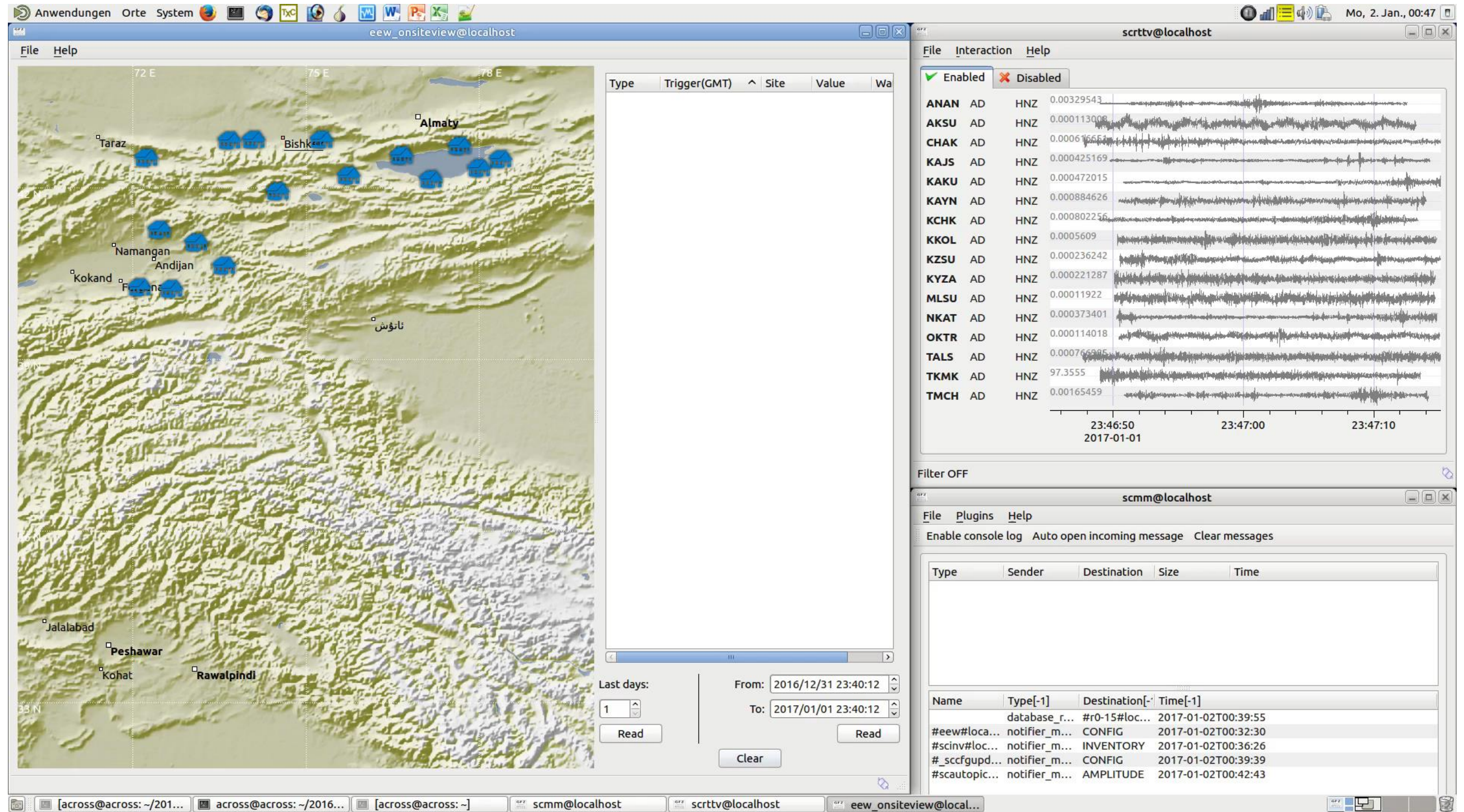
Interventi in emergenza

Percorsi difficili anche in auto

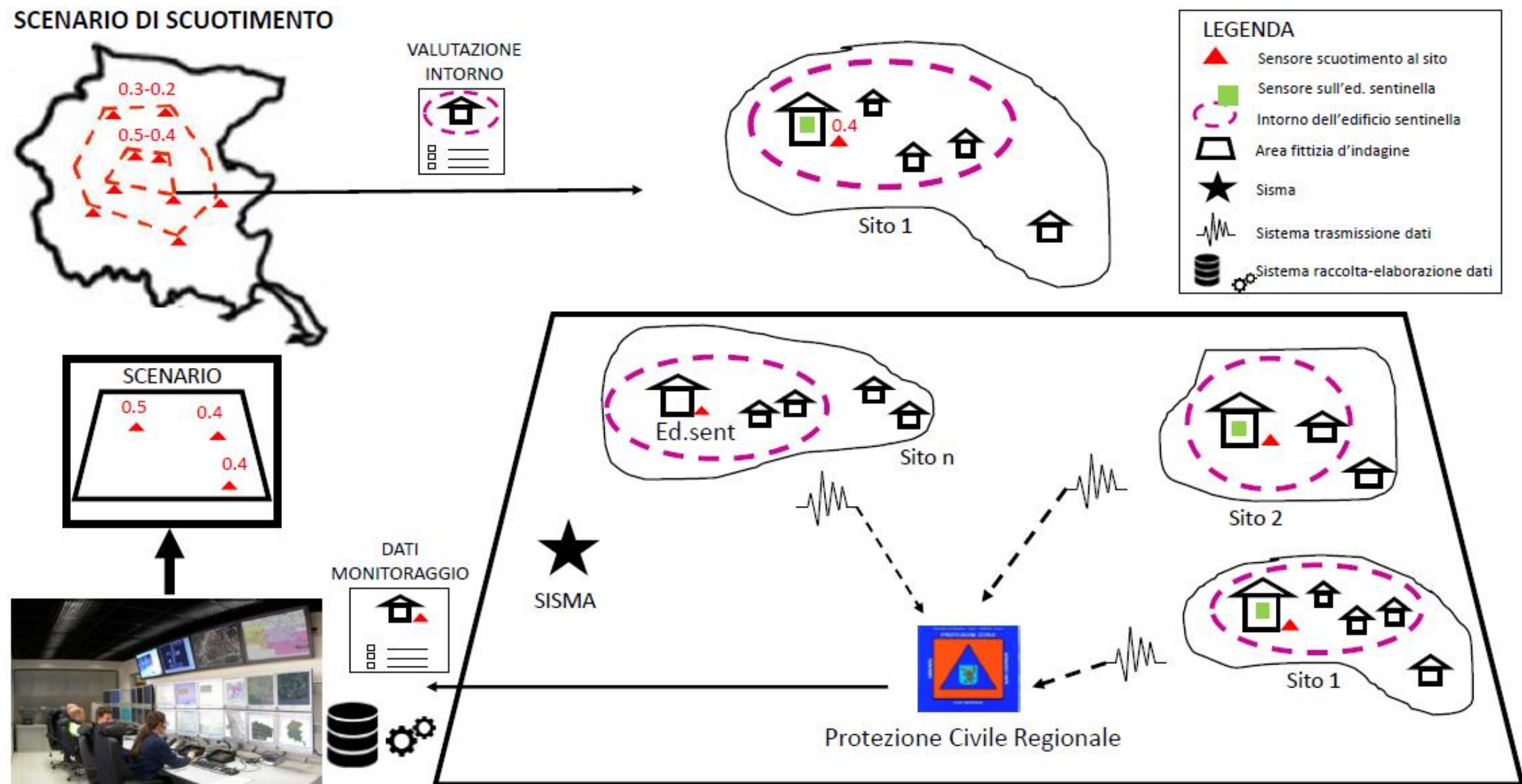


Decentralised Onsite-Early Warning

GFZ-Sentry Software, based on Parolai et al. (2015) and developed in cooperation with GEMPA GmbH.

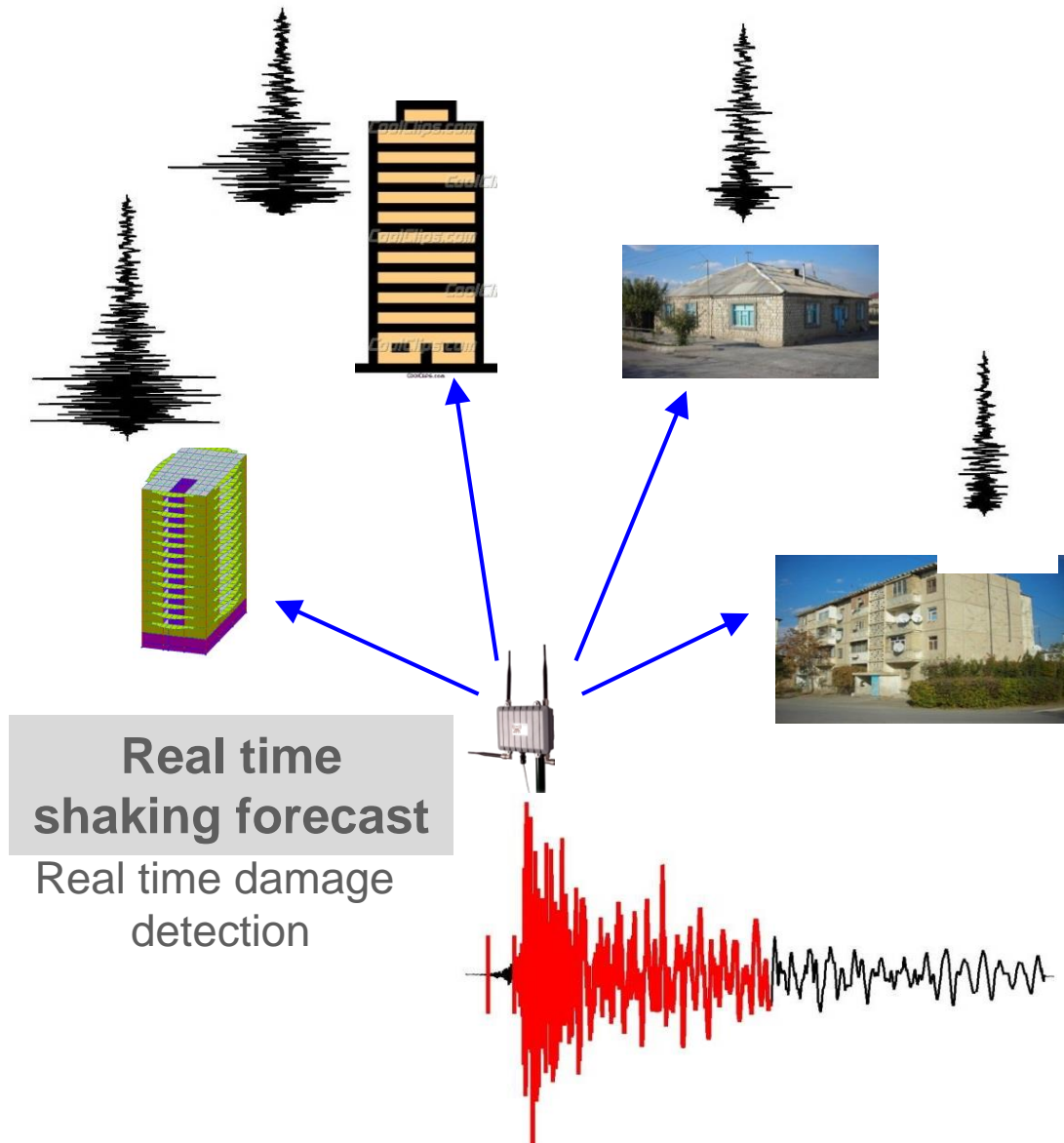


Rapid Damage forecasting in buffer areas



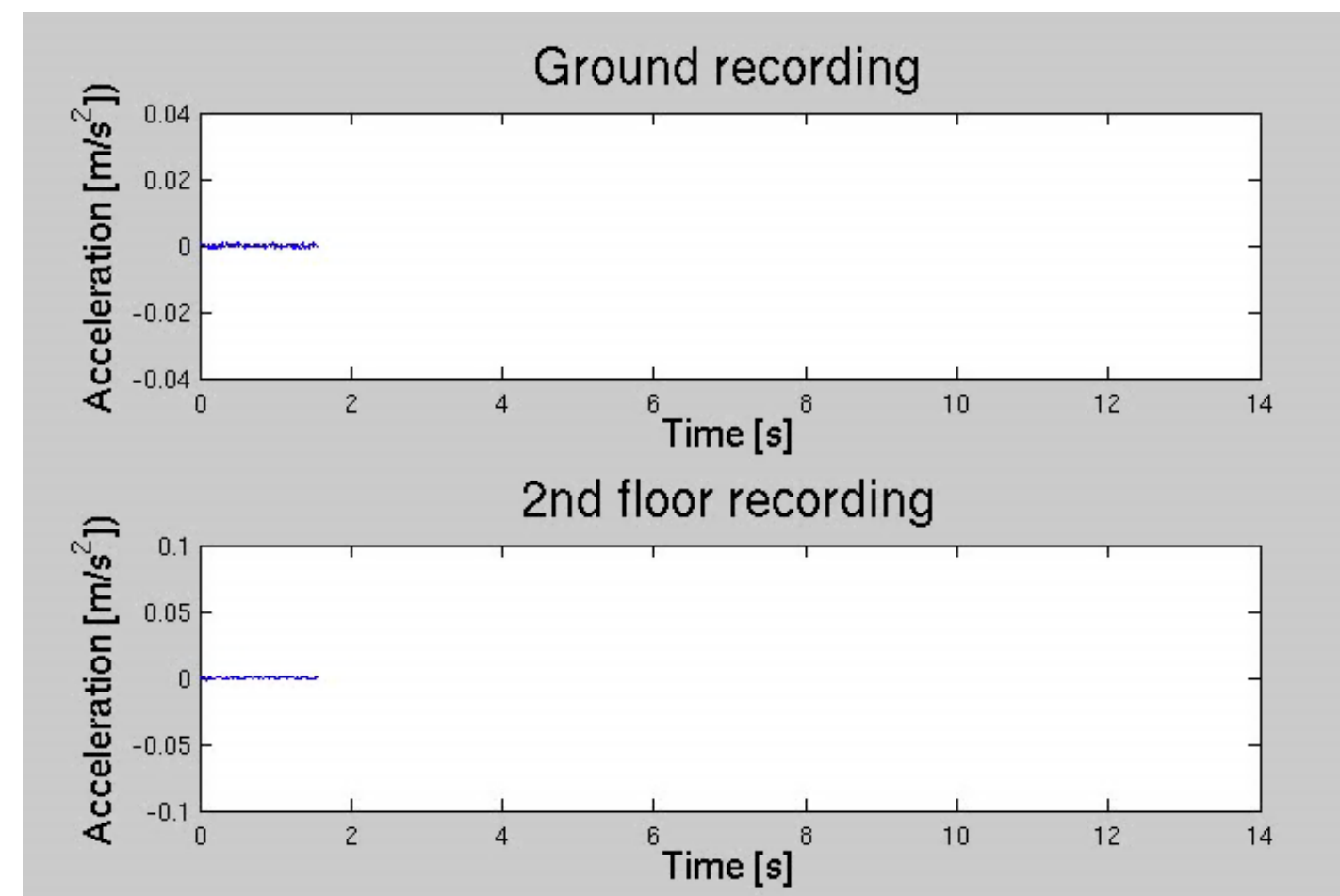
from Grimaz et al., 2017

Method 1

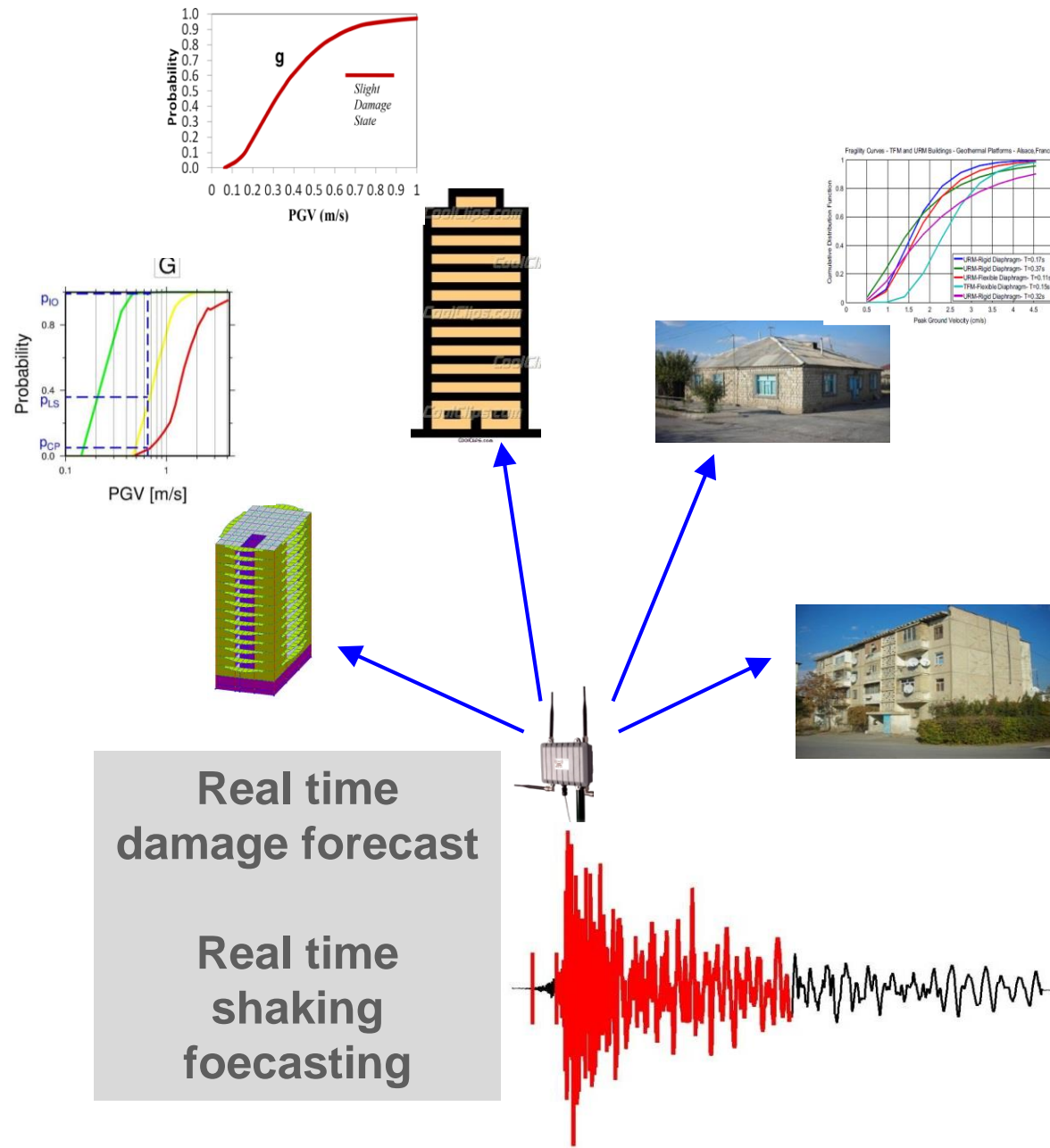


from
Parolai et al., 2015, SRL

Real time estimation of shaking for different buildings.
Input: base of one of the sentinel building
1) recording at the base of one of the sentinel building (OGS-Uni Trieste)
2) Frequency of oscillation for building type (Uni Udine)

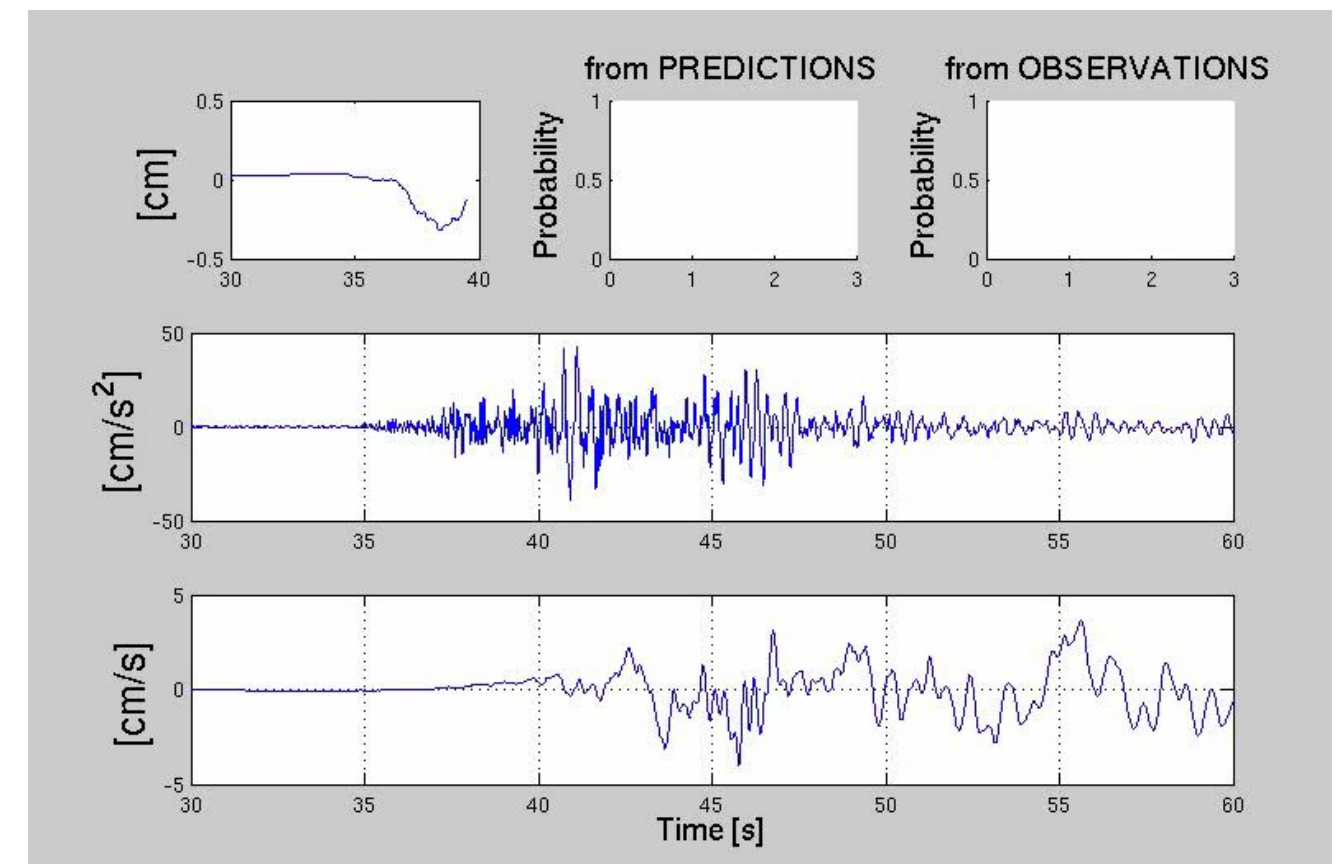


Method 2

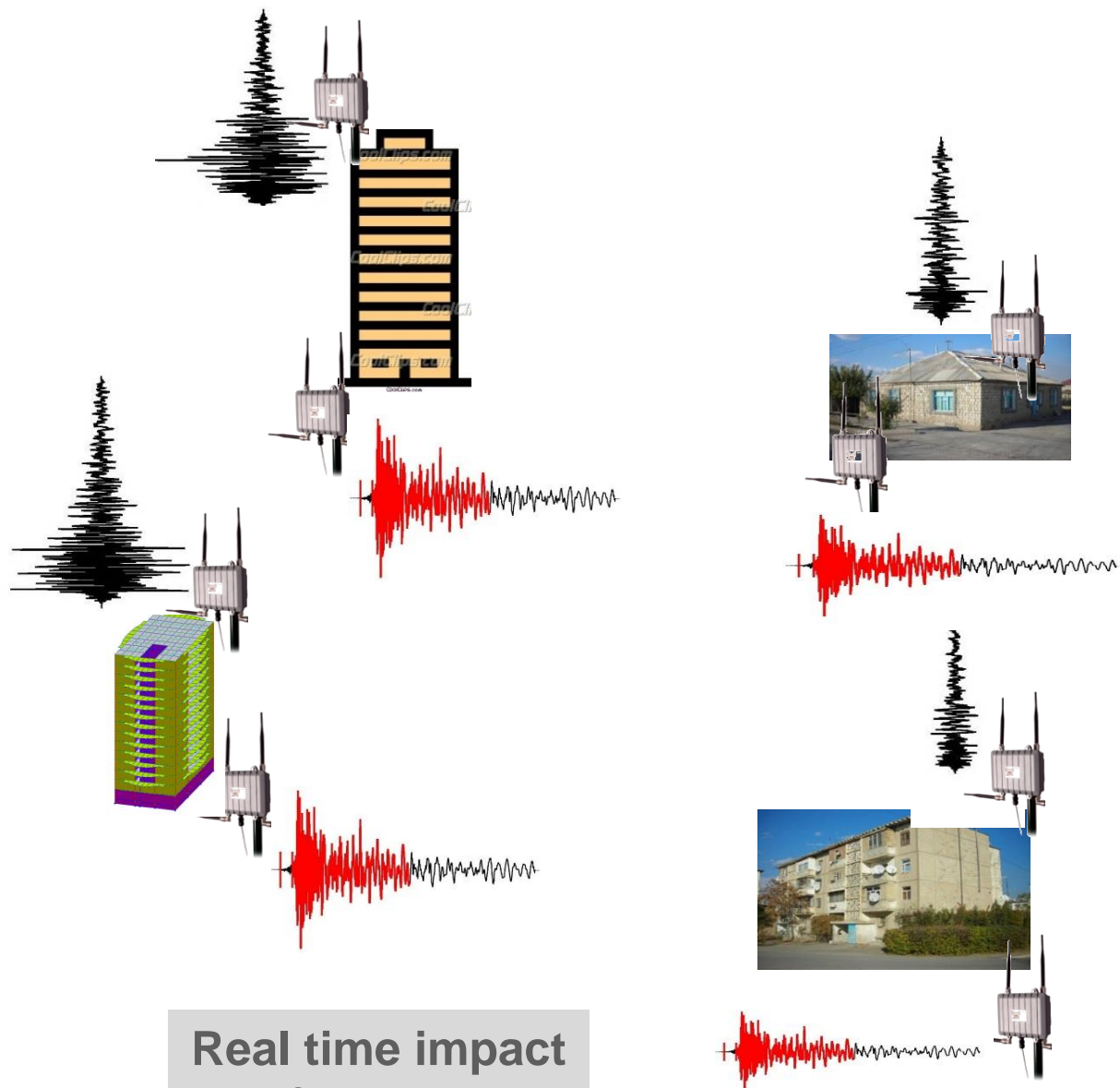


Estimation of the probability of exceedance of a certain limit state for different buildings within an area

Input: 1) recording at the base of one of the sentinel building (OGS-Uni Trieste)
2)Fragility curves for building type (Uni Udine)



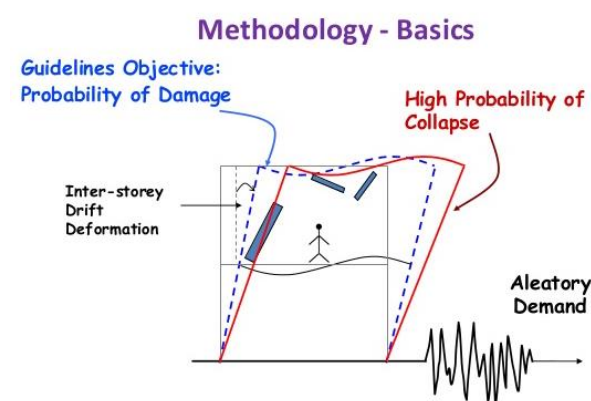
Method 3



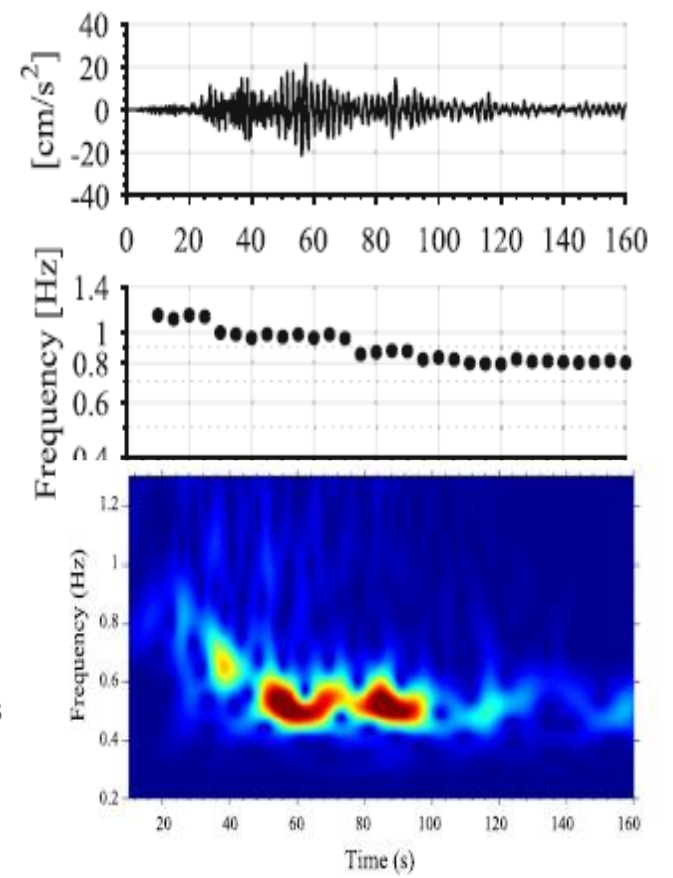
from
Parolai et al., 2015, SRL

First level estimate of possible damage in buildings with sensors at the base and at the top.

Input: 1) recording at the base of one of the sentinel building (OGS-Uni Trieste)
2) Real time measurement of interstorey-drift and/or resonance frequency variation (OGS-Uni Udine)

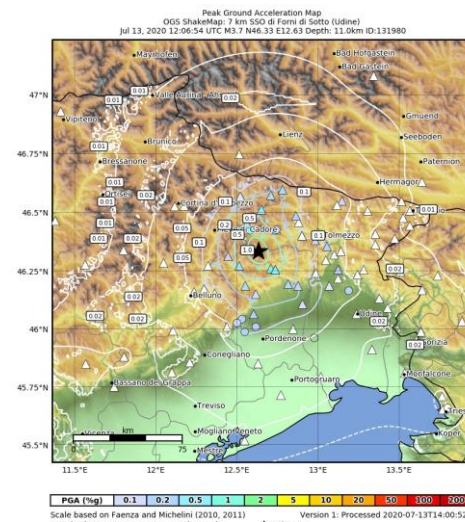
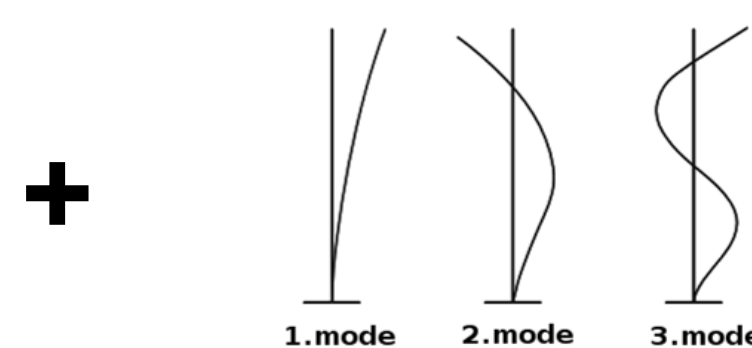


from Pianese et al, 2018



Estimating The Building's Dynamic Behavior

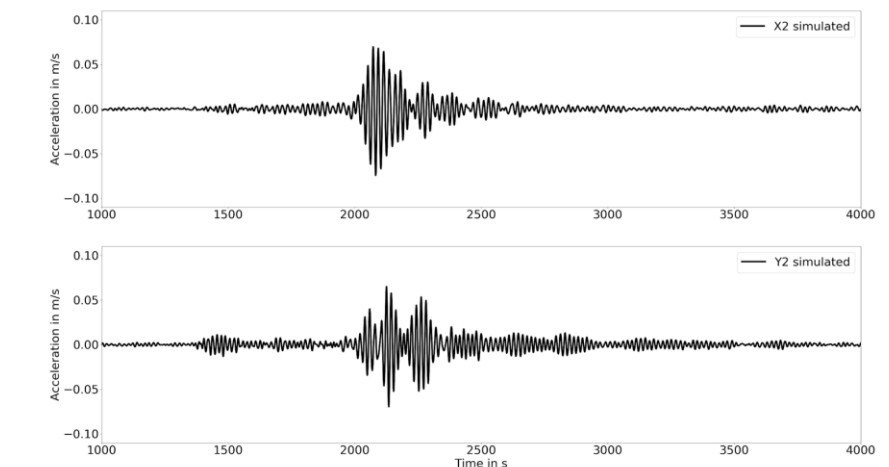
Generally, different buildings react differently to the same input ground motion. This depends on their different structural dynamic behavior, that influences expected damage.



Recordings of the M3.7 event
13.07.2020 (Tramonti di Sopra)

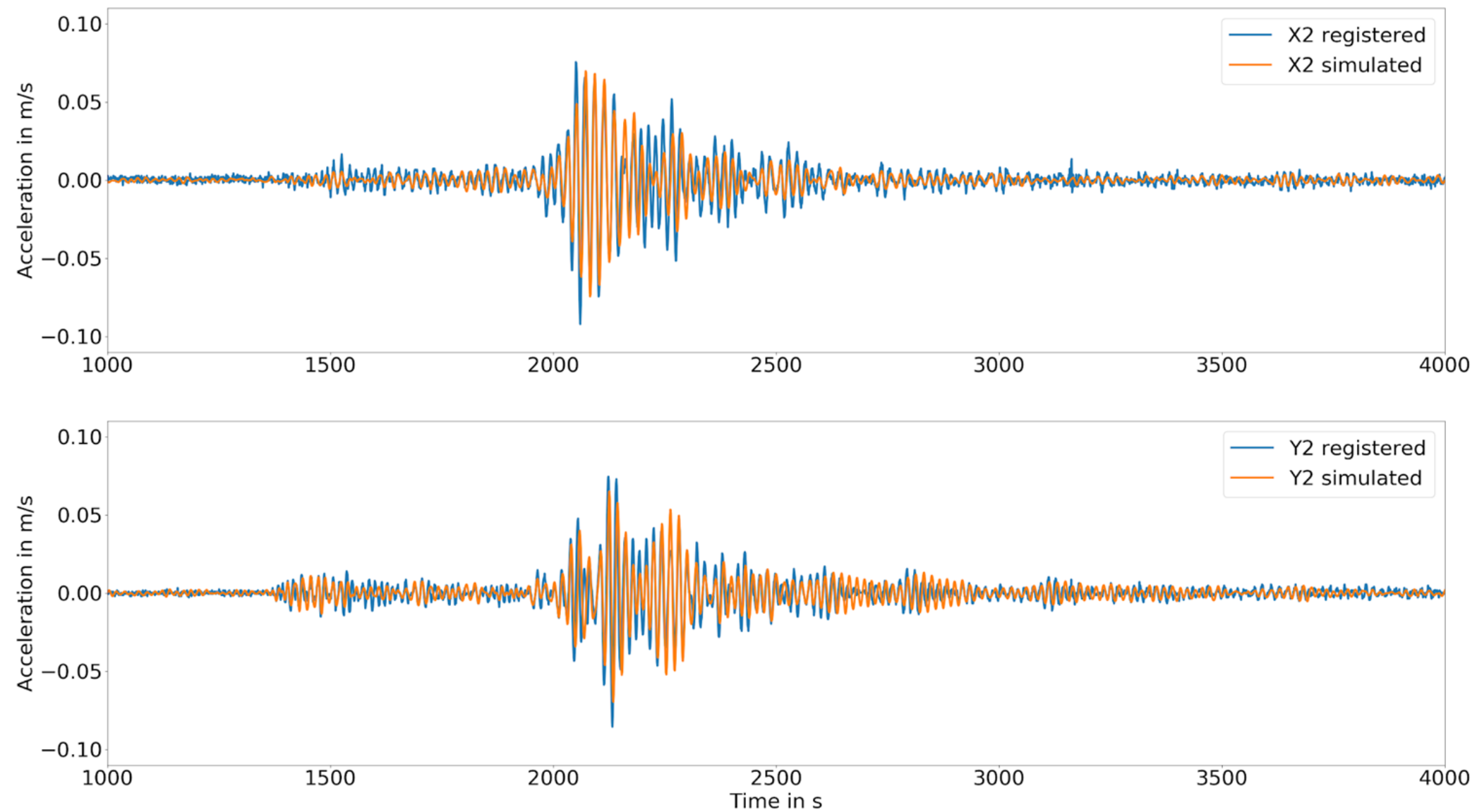


Monitored building in Aviano (UD)
characterized by noise measurements
(Sentinella/Armonia projects)

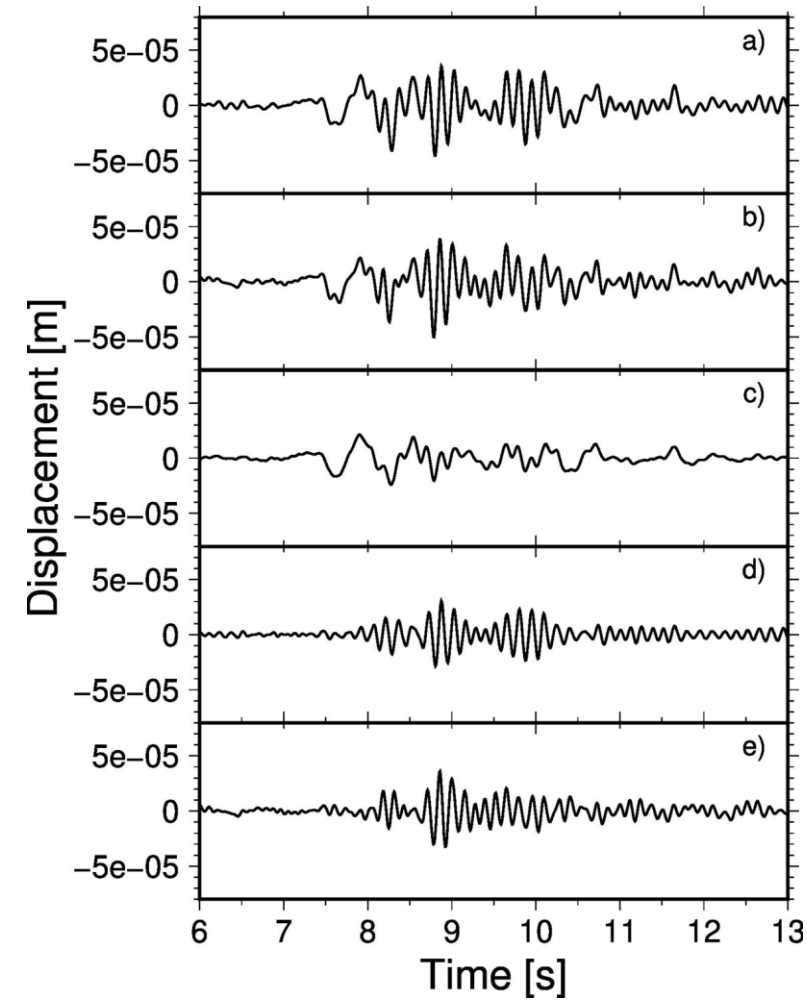
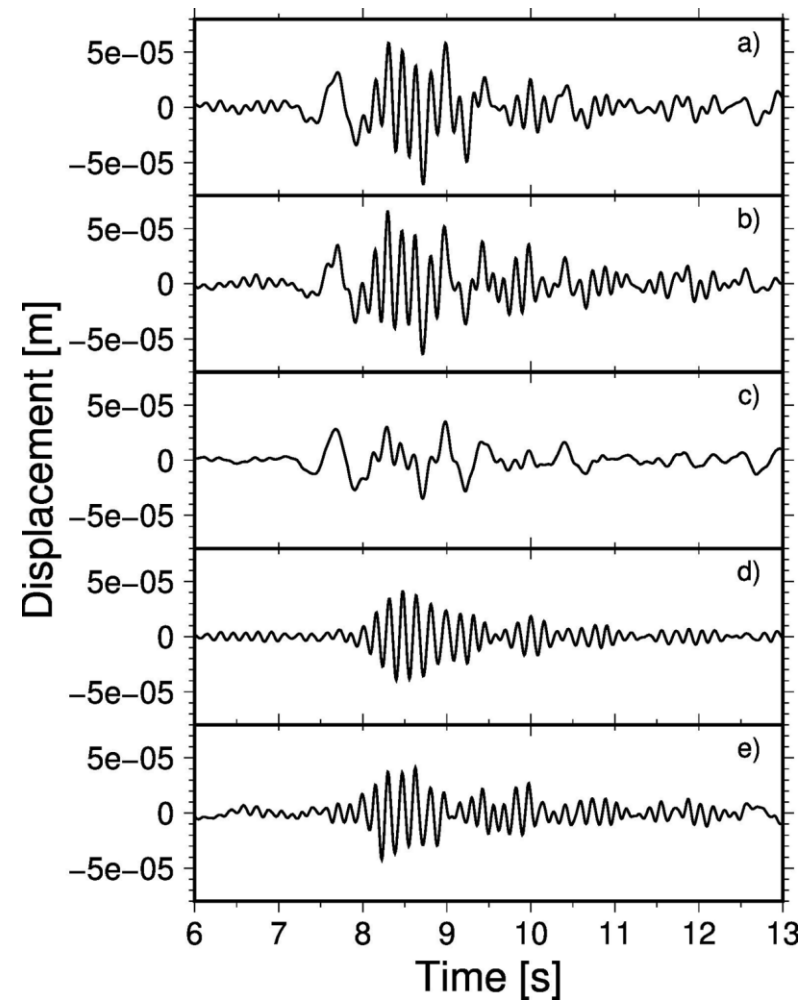


Simulated Acceleration at the top of the building

Recorded and simulated acceleration

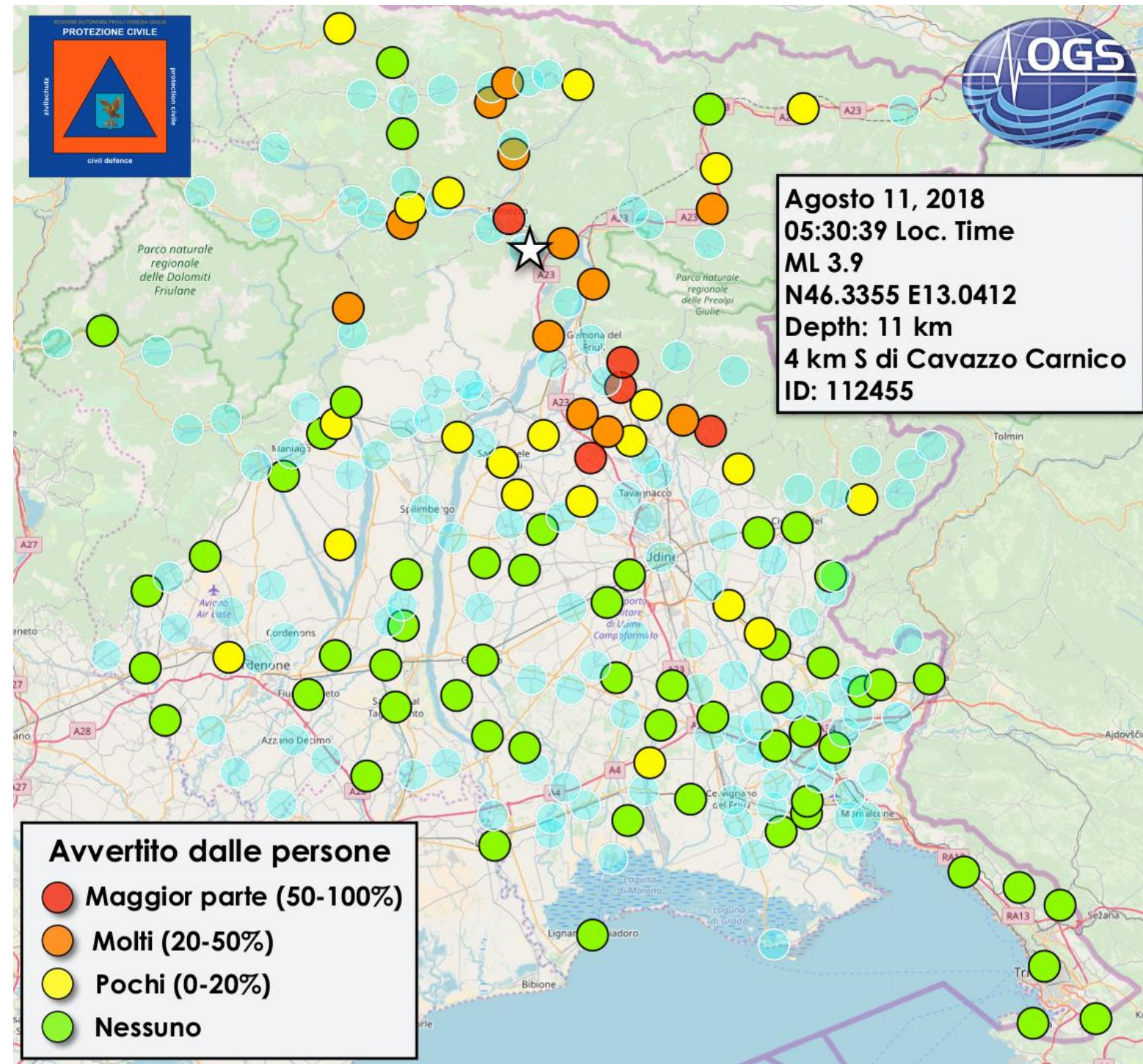


Simulated Drift and Displacement

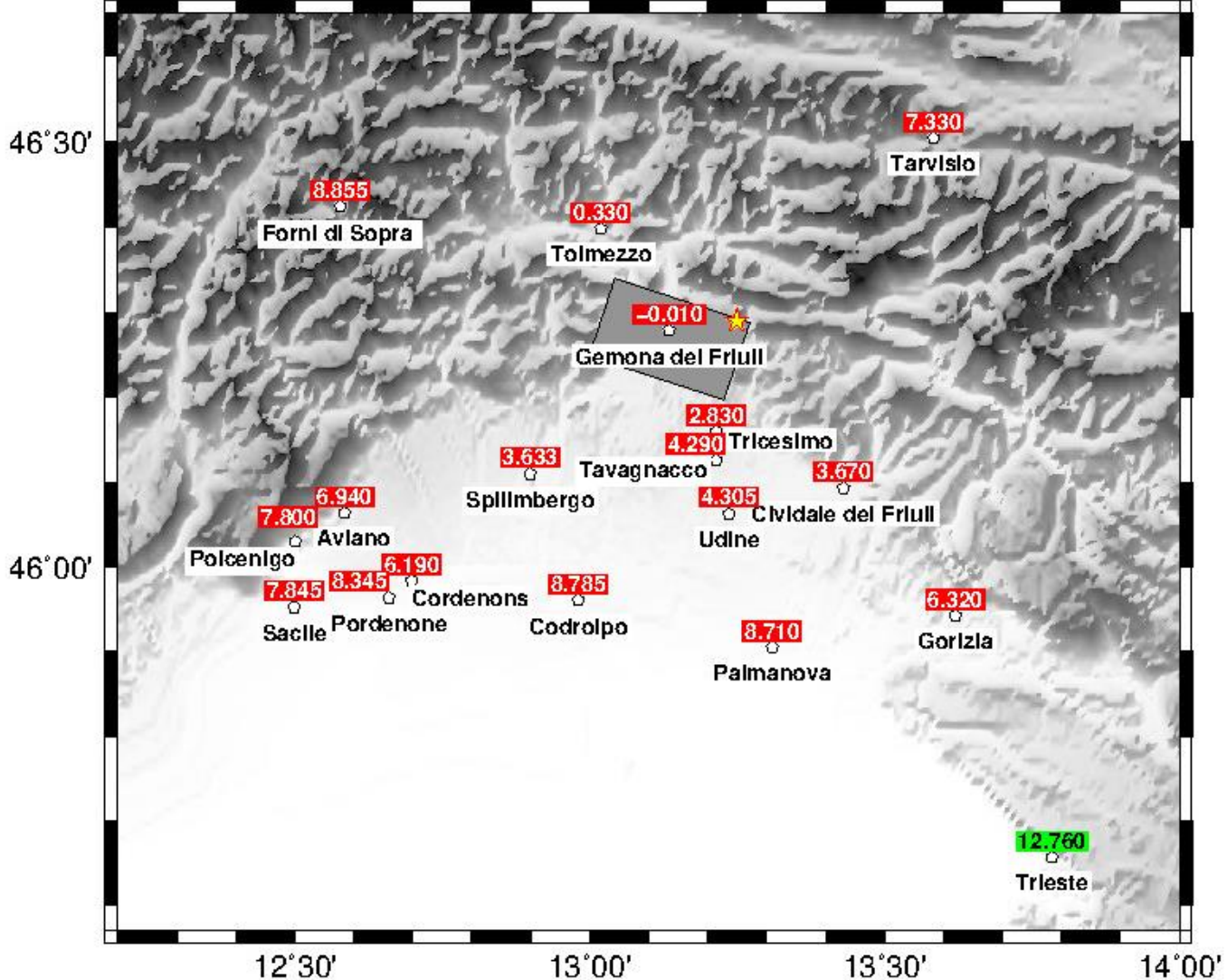


a) Simulated displacement at the top of the building, b) Displacement at the top of the building obtained by double integration of the acceleration recording, c) Displacement at the bottom of the building obtained by double integration of the acceleration recording, d) simulated drift using Z transform and e) drift calculated as difference of displacement at top and bottom. Left: x-direction, right: y-direction. Scaini et al., (2)

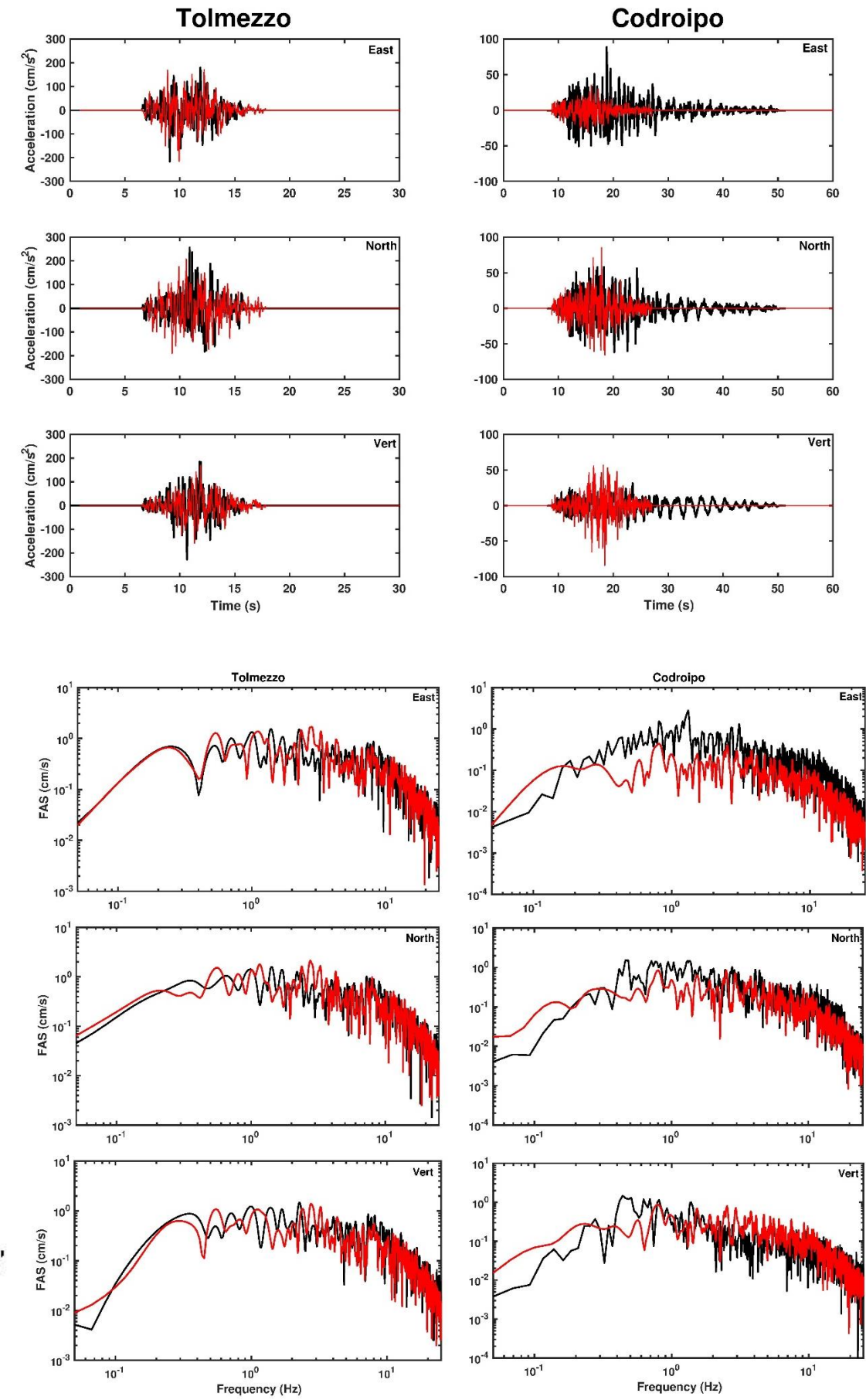
Integration of the information from seismic stations with those provided by the Civil protection volunteers: Sentinel buildings used as verification points



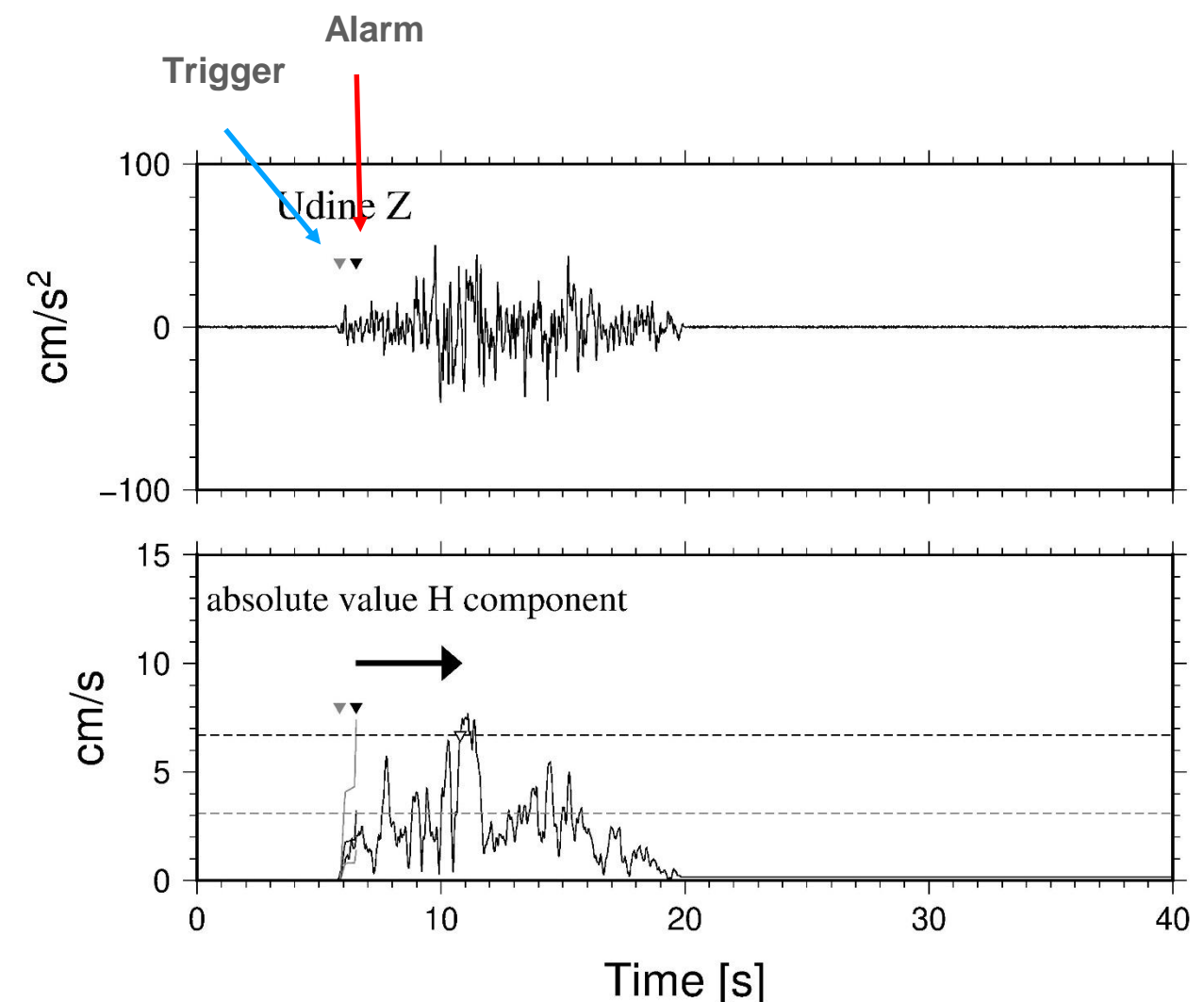
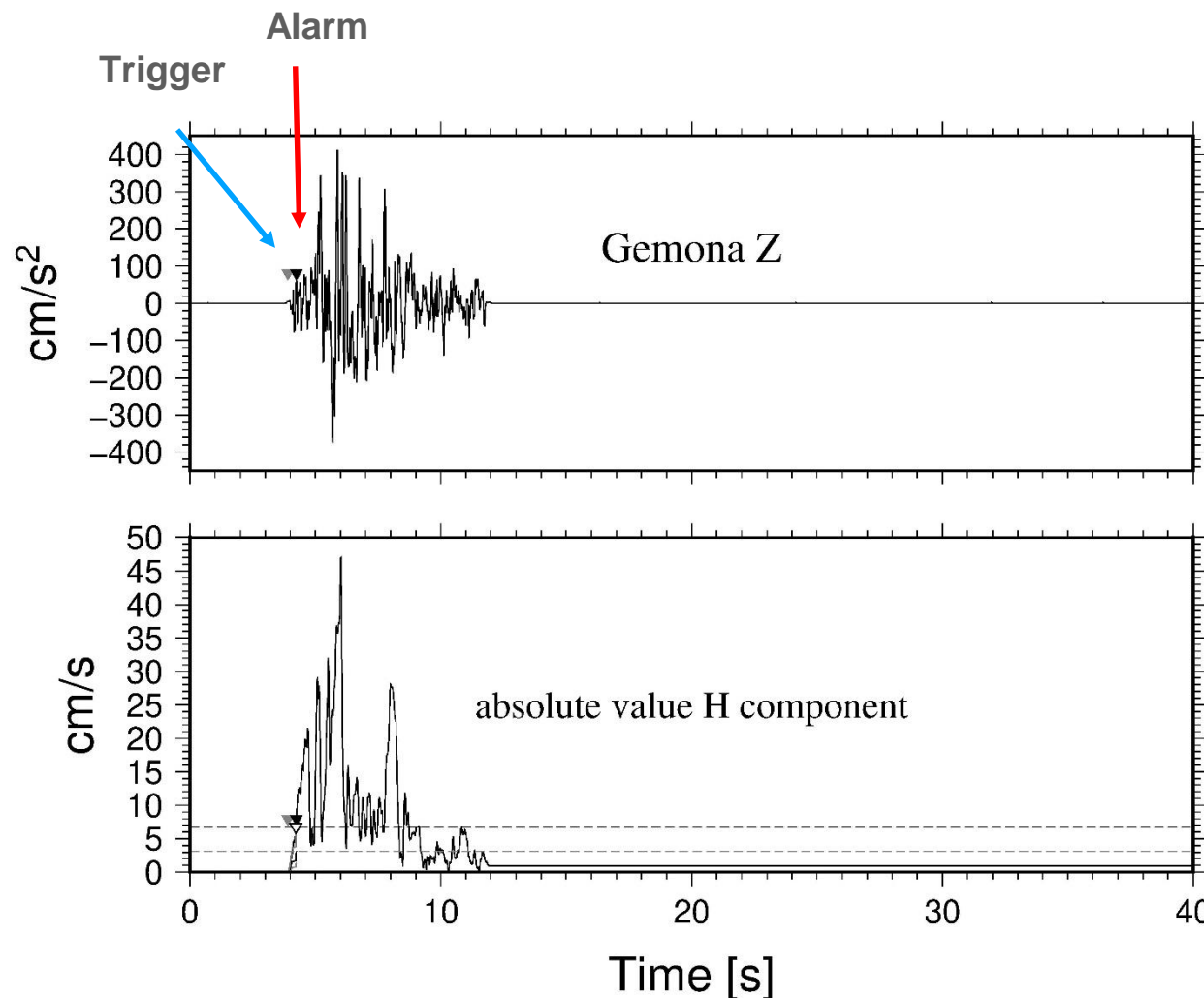
Feasibility for DOSEEW in case of repetition of the 1976 Event



from
Parolai et al., 2020



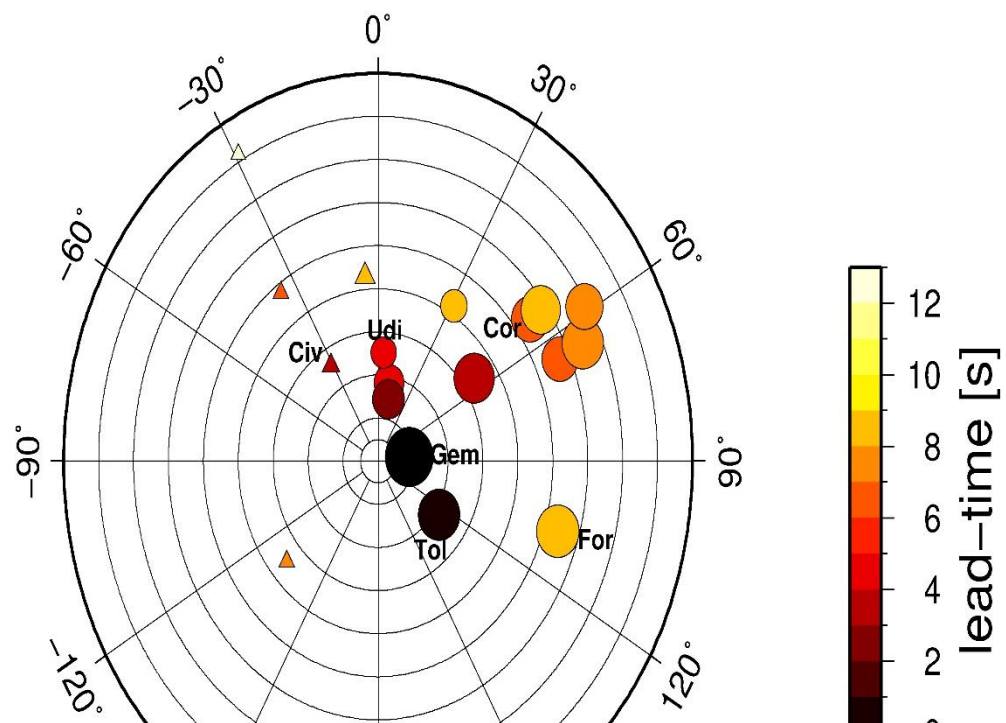
DOSEEW applied to the synthetic data



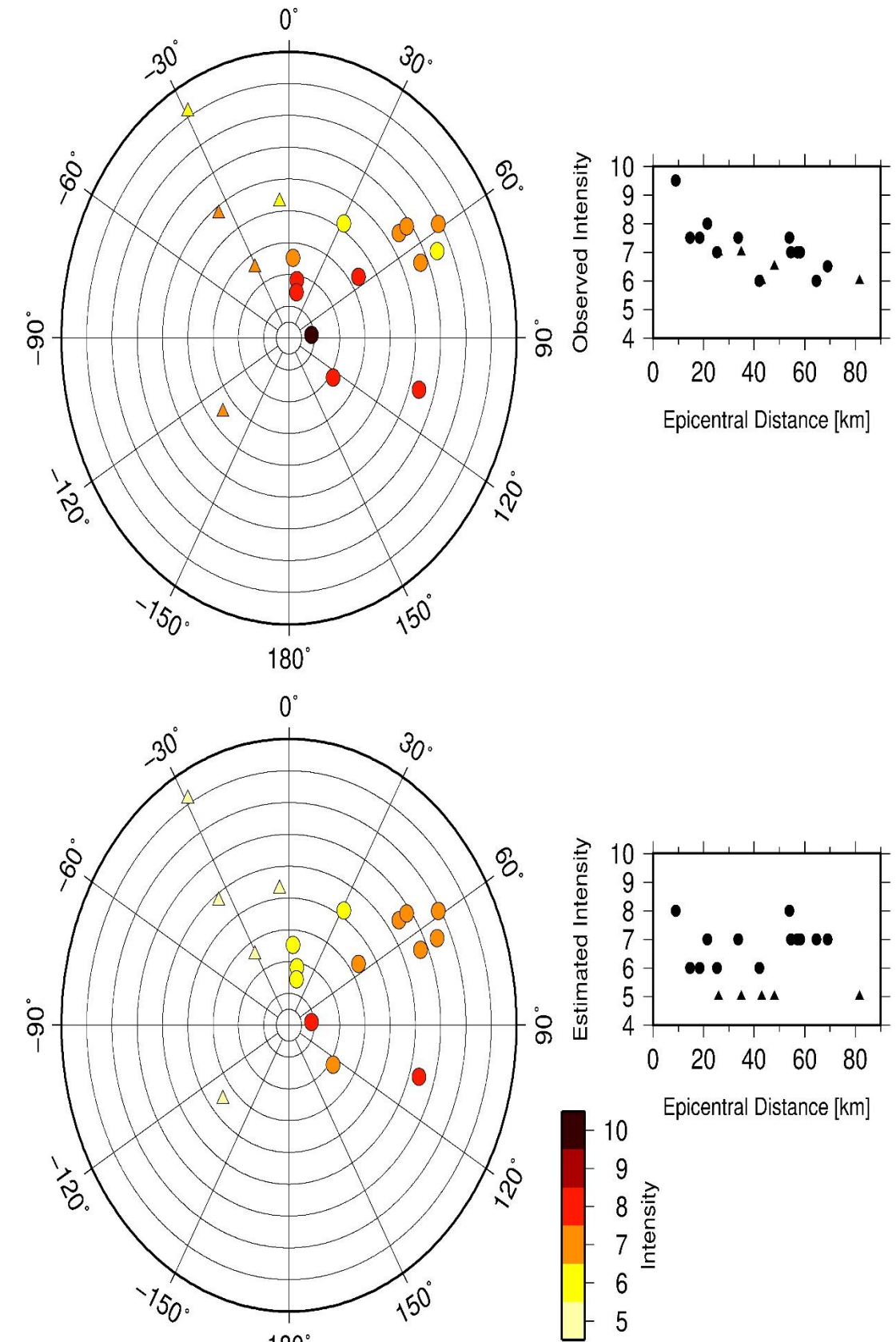
from
Parolai et al., 2020

DOSEEW applied to the synthetic data

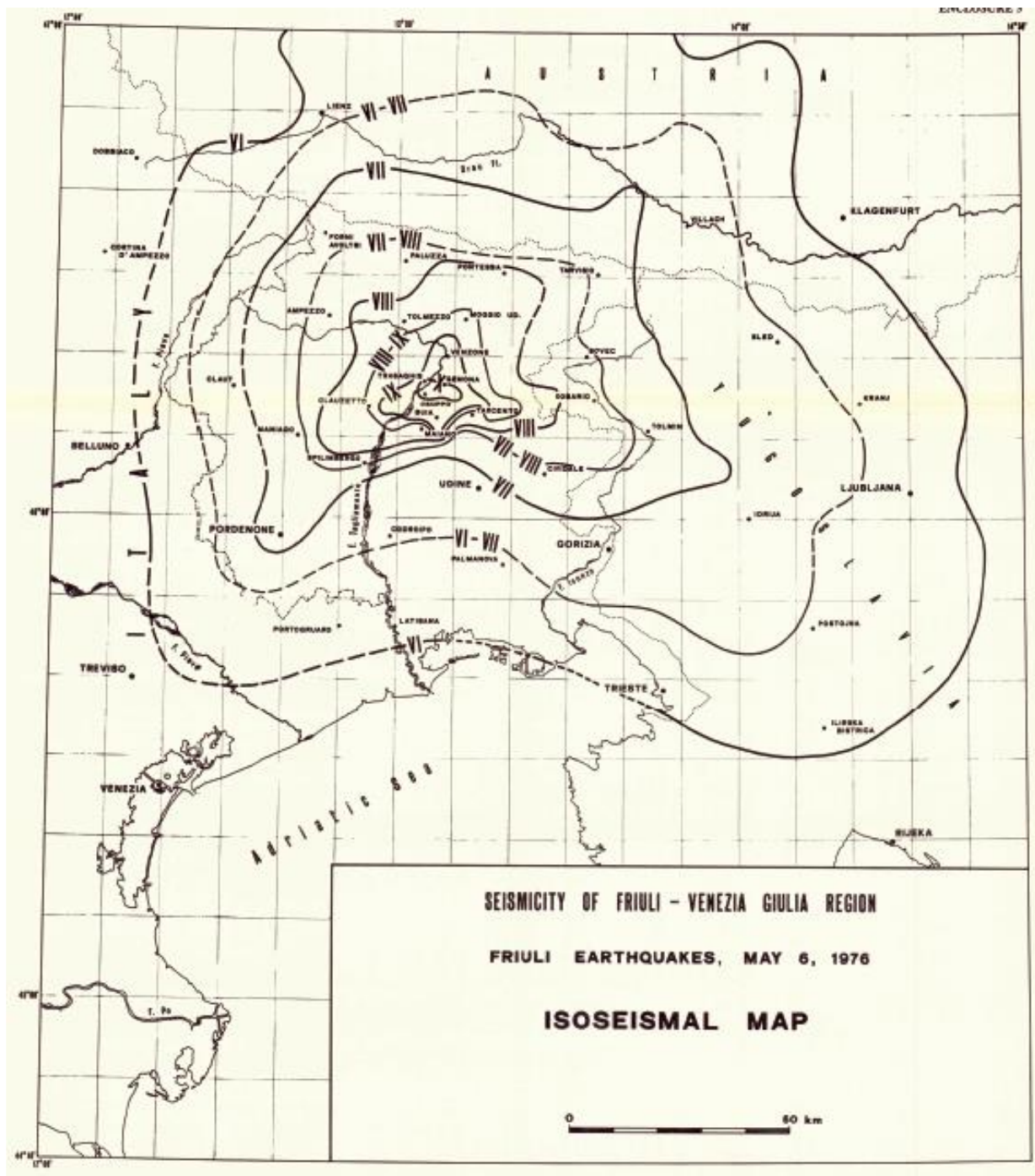
Strong dependency of lead-time on slip distribution



from
Parolai et al., 2020



Possible reduction of 10% of injured persons



from
Parolai et al., 2020

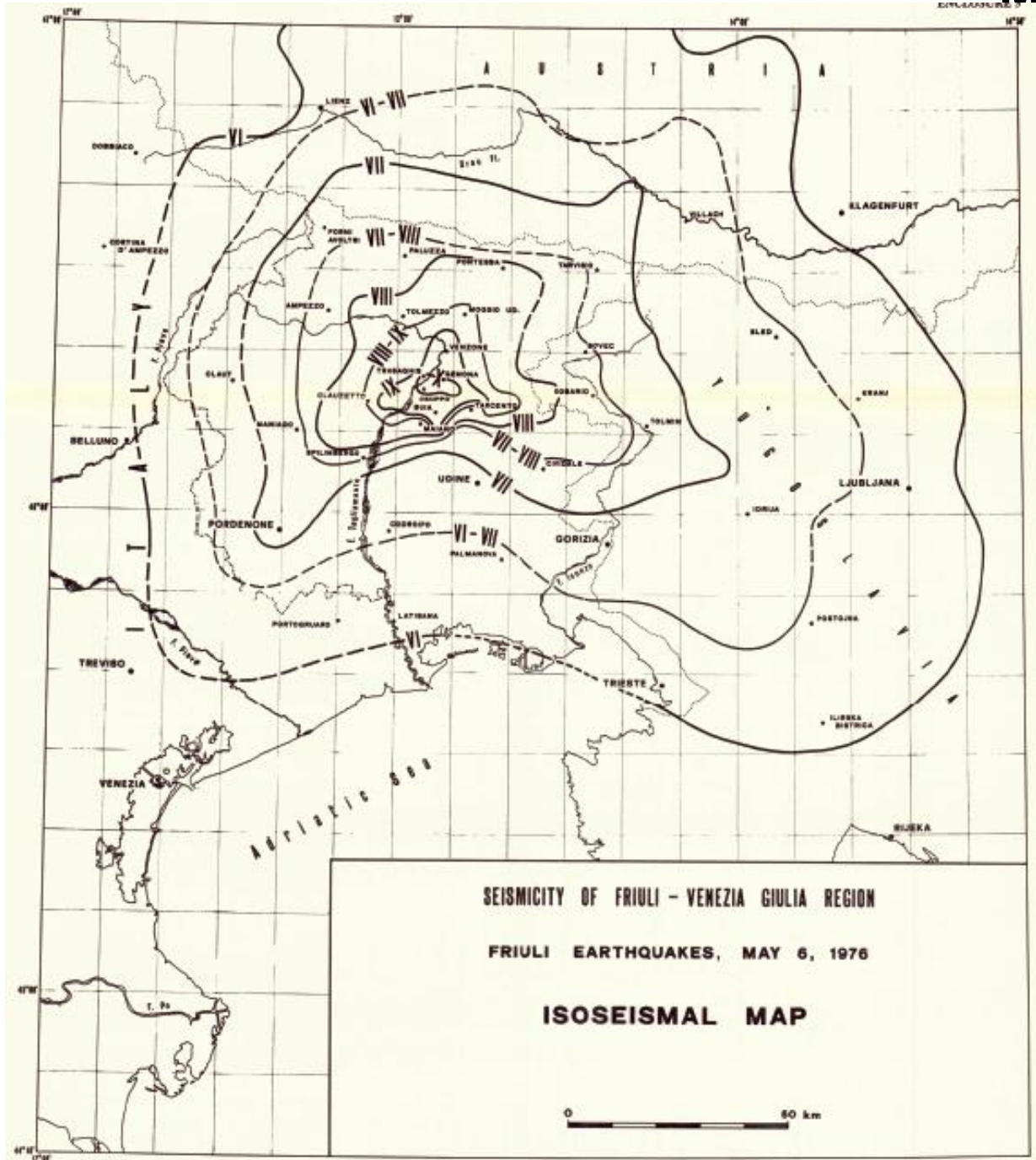
Table 1 - Summary of the localities and lead times vs injured person during the 1976 Friuli earthquake.

Locality	Lead time (s)	1976 Intensity	1976 Injured
Cividale	3.67	VII	18
Cordenons	6.19	VII	5
Tarvisio	7.33	VII	5
Pordenone	8.34	VII	27
Udine	4.30	VII	53
Forni di Sopra	8.85	VII-VIII	4
Sacile	7.84	VI-VII	6
Tavagnacco	4.29	VII-VIII	24
Spilimbergo	3.63	VII-VIII	10
Tricesimo	2.83	VII-VIII	10

Possible several seconds to stop the plant of TAL

No action was possible for this scenario for the Magnetic Marelli being in the blind zone

Magneti Marelli Automotive Lighting, Tolmezzo (UD)



from
Parolai et al., 2020



- production of electronic components for LED lights
- 5.000 m²
- > 1100 employees

TAL – Transalpine Pipeline



- Italy, Austria and Germany
- 40% of the energy needs of Germany and the Czech Republic, and 90% of Austria
- 753 km
- 7500 m³/h
- 750 employees involved
- 1.2×10^9 €